Infrared medical thermography, medical applications, and its basic principles: a review

Ali Faisal Abdulkareem[1*] and *Auns* Qusai Hashim[1]

[1] Al-Nahrain University, College of Engineering Biomedical Engineering Department, Baghdad, Iraq

Abstract. This narrative review aims to summarize in one paper all the known applications of infrared (IR) in medical thermography, medical applications, and the standardization protocols and basic conditions for thermal imaging in diagnostic medicine until December 2023.This technology primarily harnesses naturally emitted IR radiation from the subject's surface. These IR radiations emitted from the human body surface have been used in different fields of medical imaging to diagnose different kinds of diseases, disorders, and congenital anomalies and aid in medical therapy. Thermal imaging is a non-invasive, non-contact diagnostic technique used to measure the temperature of the human body. Therefore, IR thermal imaging has drawn significant attention and interest in recent years in a broad range of commercial applications due to its unique and superior properties. This commercial development has been supported by fundamental and applied research studies.

Introduction

Human body imaging has become a vital condition for improving medical diagnosis. A lot of techniques are used to start, such as X-ray imaging, ultrasound imaging, magnetic resonance imaging (MRI), and other technologies such as histogram colors contrast seed point selection (HCC-SPS) [1]. Since the 1940s, infrared detectors have become increasingly sensitive and accurate. First-generation detector arrays, which include photon detectors such as lead sulfide (PbS), were the first practical IR detectors sensitive to infrared wavelengths reaching to 3 m. Between the end of the 1940s and the beginning of the 1950s, lead selenide (PbSe), lead telluride (PbTe), and indium antimonide (InSb) were sensitive to infrared wavelengths up to 3-5 m in medium wavelength IR (MWIR). The end of the 1950s saw the first semiconductor alloy material with a group II-VI tunable bandgap, such as MCT (HgCdTe). Linear array technology was first achieved in PbS, PbSe, and InSb detectors when it became obtainable in the beginning of the 1960s. During the seam period, it was utilized to create IR sensor arrays via photolithography. The advent of single-crystal InSb material marked the beginning of the development of photovoltaic (PV) detectors. By enabling long - wave infrared (LWIR) forward-looking imaging radiometer (FLIR) systems to run at 80K on a single - stage cryoengine in the late 1960s and early 1970s,MCT photoconductive detectors greatly reduced the size, weight, and power consumption of these systems. Innovative platinum silicide (PtSi) detectors were made possible

* Corresponding author : alialbeldawi79@gmail.com

by silicon technology, and now days, PtSi detectors are widely used in MWIR high-resolution applications and are standard commercial goods. In the late 1960s, Second Generation Detector Arrays were introduced, which witnessed the invention of charge-coupled devices (CCDs) with on-focal-plane electronic analogue signal readouts that could multiplex the signal from a very large array of detectors. Monolithic extrinsic silicon detectors were demonstrated first in the mid-1970s. Then, in the late 1970s through the 1980s, MCT technology efforts focused almost exclusively on PV device development because of the need for low power and high impedance for interfacing to readout input circuits in large arrays. This effort has paid off since the 1990s to provide large 2D arrays in linear formats. These detectors use Time Delay Integration (TDI) for scanning systems; in staring systems, they are offered in rectangular and square shapes. [1][2].

However, the complex system of heat regulation in the human body was not well understood until the early 20th century [3]. When Dr. R. Lawson, a surgeon, noticed that his patients with breast cancer had warmer skin around the cancerous region, medical thermography was started in the 1957[4]. In the publication, Ring conducted research on quantitative infrared thermography 23 years ago (Ring 1990). [5]. The COVID-19 pandemic outbreak in 2019 pushed for the development of infrared thermography technologies as a primary diagnostic tool for the disease, as they may identify feverish states and lung infections [6].

In 2019 [10], Ricardo Vardasca et al. investigated infrared thermal (IRT) imaging, a modality that allows non-invasive and non-ionizing monitoring of skin surface temperature distribution, providing underlining physiological information on peripheral blood flow, the autonomic nervous system, vasoconstriction / vasodilatation, inflammation, transpiration, or other processes that can contribute to skin temperature.

In 2016 [4], Urakov A et al. revealed the symptoms of a healthy and flat foot after short-term load applying infrared thermography. Thermal images of the subjects' feet were obtained after they had stood on one leg for 30 seconds, keeping body balance on a flat horizontal surface. Infrared monitoring was performed using a Thermo-Tracer TH9100XX (NEC, USA) thermal imager. It was determined that a zone of local hyperthermia appears on the line connecting metatarsophalangeal joints and moves medially in patients with flat feet. The average temperature in the medial part of the line increases by 0.1°C and more compared to the average temperature of the lateral line.

1 IR Thermography Overview:

1.1 History of IR Thermography Development in Medical Field:

There has been much research and investigation into the development of IR imaging systems. Czerny documented the first infrared image of a human subject in Frankfurt in 1928 [1][2]. The 1940s saw the development of the first infrared imaging devices, which were made accessible to manufacturing and healthcare in 1959. In order to image the increased heat over arthritic joints, the Pyroscan, an equipment dating back to 1942, was first utilized in Bath in 1959. Though it took three to four minutes to acquire each image and was nearly impossible to quantify, the Mark 2 equipment produced better-quality pictures. Later, with more advanced technology, more dynamic (and objective) images were produced, which could be a helpful addition to radiological studies [3][4].

In Europe, the United States, and Japan, a new generation of thermal imaging systems was created in the 1960s and 1970s. Electronic isotherms were included in the picture, and oscilloscope displays were introduced. In the 1960s, the first color thermograms were created utilizing multiple-exposure color photography. The mid-to-late 1970s saw the introduction of mini-computers for image processing, which offered color displays, image analysis, and most

importantly, data and picture storage. With this, quantitative thermography was born [5]. Focal plane array detectors with high-speed pictures at high thermal and spatial resolution are used in modern systems that have been introduced in the previous three years. The quality of photographs has significantly increased; the crude clinical photos from forty years ago are no longer comparable to modern digital thermograms.

Nowadays, rheumatology is used for the quantitative investigation of inflammation and anti-inflammatory medications, Raynaud's phenomenon, sympathetic disruptions, pain syndromes, peripheral circulation problems associated with connective tissue diseases, and locomotor injuries [6].

From a modern perspective, the early infrared cameras lacked many features, including stability, repeatability, precise measurement, and a high degree of geometric and thermal resolution. However, as initially employed by Lawson [2][7]. they permitted recording the measurement data without coming into contact with or tampering with the measured skin. The LN2 cooled MCT scanner Icotherm, created by Carl Zeiss Oberkochen in the mid-1980s, was a medical first for many years. Sadly, its high cost made it inaccessible for doctors and clinics.

The AGA thermo-vision equipment Figure 1, which were the medical standard for a long period, were largely utilized by them and were significantly cheaper. Since 1983, Berz [2][8] has utilized both cameras.

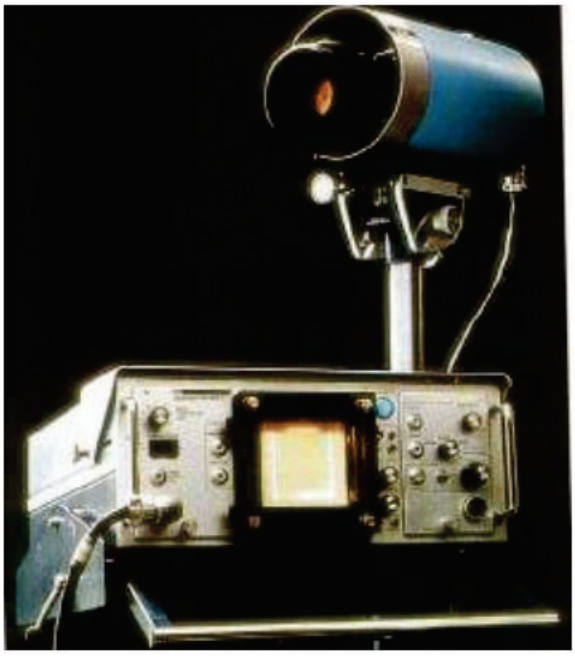

Fig. 1. One of the medically broadly used AGA Thermo-vision cameras (AGA 680 medical, ca. 1975)[2]

An "explosion" of IR camera models and manufacturers—which were also employed for medical purposes—marked the latter two decades of the 20th century. Despite typically being based on scanning MCT sensor systems, their technology is quite sophisticated. Figure 2 illustrates how noise, a fixed pattern, thermal drift, and numerous other instabilities plagued the first infrared cameras using a completely new technology, known as uncooled focal plane array (FPA) microbolometer cameras, when they were originally introduced for medical applications compared with clear cooled MCT sensor system.

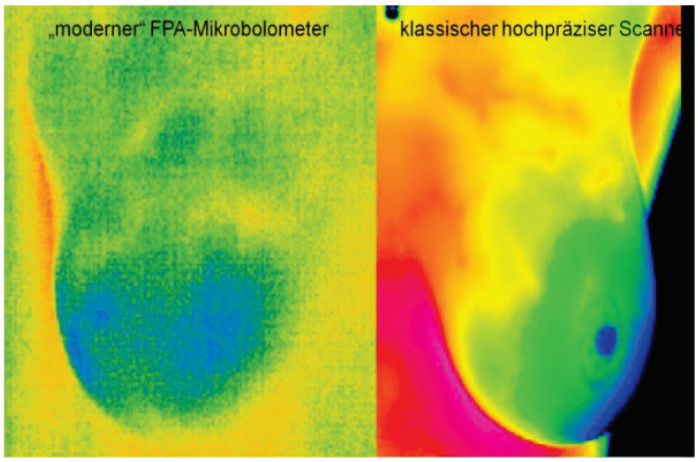

Fig .2. Image of an early uncooled FPA microbolometer camera, compared to cooled MCT scanner (both built in the late 1990s)[2].

Finally, abnormal body temperature is a natural indicator of illness [9], and modern uses of infrared thermography for medical diagnosis include rheumatology, cancer, allergy disorders, angiology, plastic surgery, and other fields. Modern thermal imaging has to be carried out in accordance with specific guidelines to ensure results are dependable and repeatable [10]. Recently, in 2017, IR used a 3D dynamic thermography system for biomedical applications [11].

1.2 IR Thermography standards:

Infrared cameras track temperature changes over the viewable surface as thermal energy spreads via diffusion beneath the surface. As a homogeneous material, it follows that given a surface that is uniformly heated, the temperature distribution is also uniform. Variations in local surface temperature are the result of a fault obstructing the heat flow at a specific depth. Parameter DT can be used to assess a defect's visibility [12]:

$$D_T = \left|\frac{\Delta T}{\Delta T_S}\right| = \frac{|T_S - T_d|}{|T_S - T_r|} \quad (1.2)$$

Where:

Td is the temperature over a defective zone

Ts is the temperature in a sound zone

Tr is a reference temperature

1.3 Standardization protocols for thermal imaging in medicine:

The use of a thermography camera for fever screening has been defined by two guidelines released by the International Standards Organization (ISO). The first step, published in September 2008 (IEC 2008), outlines the standard design and performance characteristics of a radiometric infrared camera for screening, where variations on the face can be a little more than one degree Celsius. The second step, published in March 2009 (ISO 2009), specifies the recommended deployment mode and includes system testing and user training. Clinical protocols include preparation of the patient, positioning of the body for image recording, and thermography evaluation [13]. As an example, the University of Glamorgan developed the Glamorgan Protocol

for recording and evaluating thermal images of the human body. The "Atlas of Normal Skin Temperature Distribution" project was initiated with the goal of filling in the knowledge gap regarding the skin temperature distribution of healthy people. The idea was to portray as much of the relevant anatomical region as you could. Anatomical landmarks were positioned in relation to the image's edge in each view to accomplish this. Thus, regardless of the subject's body percentage being scanned, an identical view of the body region was obtained. These definitions aim to reproduce the views of body positions as accurately as possible and, in that way, increase thermal imaging reproducibility [14].

2 IR Applications in Medical Field.

2.1 IR Thermography in Lesion Detection.

IR proved to be an effective tool to detect lesions and aid in determining if they are malignant or benign, such as:

2.1.1 Cutaneous melanoma metastases.

In the 2013 study by Amber L. Shada MD et al., images of 251 visible lesions were taken from 74 patients (38 men and 36 women). Using either a clinical diagnosis or pathologic confirmation, the diagnosis was made. Subjective observations have shown that melanoma metastases appear warmer than comparable benign tumors. Infrared (IR) thermography was expected to be sensitive and selective in differentiating palpable melanoma metastases from benign lesions, as Figure 3 below illustrates. With a sensitivity of 39% and a specificity of 100%, it could identify the malignancy of tiny (0–5 mm) lesions. There was 58% sensitivity and 98% specificity for lesions larger than 5 to 15 mm. Lesions larger than 15–30 mm had a sensitivity of 95% and a specificity of 100%; lesions larger than 30 mm had a sensitivity of 78% and a specificity of 89%. Figure 3 below also illustrates the positive predictive value of 88%–100% for all strata and the negative predictive value of 95% for lesions >15–30 mm and 80% for lesions >30 mm [15]. These results were confirmed by another study by Lese et al. in 2022 which show similar results [16].

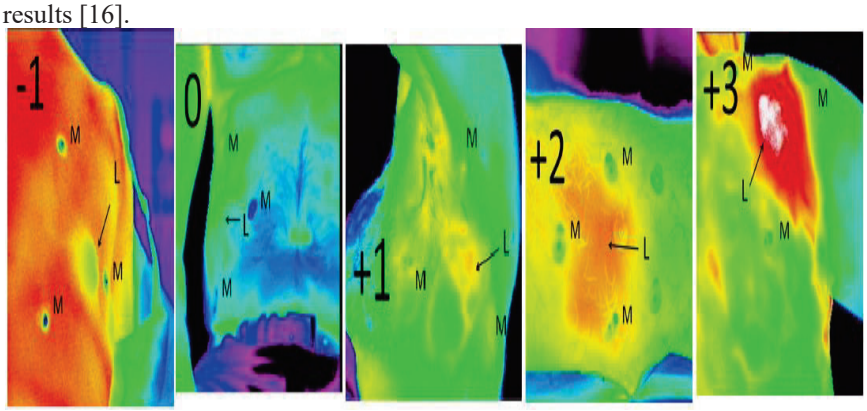

Fig .3. A graphic illustration of the study's scoring methodology. L indicates the location of the lesion, and M indicates the locations of the metallic markers. By comparing the score to the surrounding tissue, the IR intensity of the lesion is ascertained [15].

2.1.2 Breast cancer pre-diagnostic.

In 2018, Sebastien Jean Mambou et al. reviewed several papers exploring infrared digital imaging, and these authors realized that an infrared image processing-based computer-aided diagnostic (CAD) would be impossible without a model like the well-known hemisphere model. They conducted a comparative analysis of several breast cancer detection methods using potent computer vision techniques and deep learning models, coming to the conclusion that computer scientists' perspective on breast cancer thermography detection could be a useful addition to the field. In 2020, Samir S. Yadav and Shivajirao M. Jadhav found that inflammation and blocked areas that predict cancer may be detected by thermography. The precancerous tissues and the regions surrounding breast cancer always exhibit higher thermal activity when compared to a healthy breast. A major benefit of medical testing is that it can be utilized before any obvious symptoms appear. This research uses machine learning (ML), a statistical technique that allows software programs to learn from data without having to be explicitly coded. ML can assist with this by understanding these thermal scans and pointing out possible regions that require further investigation by a physician, as illustrated in Figure 4 [17], [18], [19].

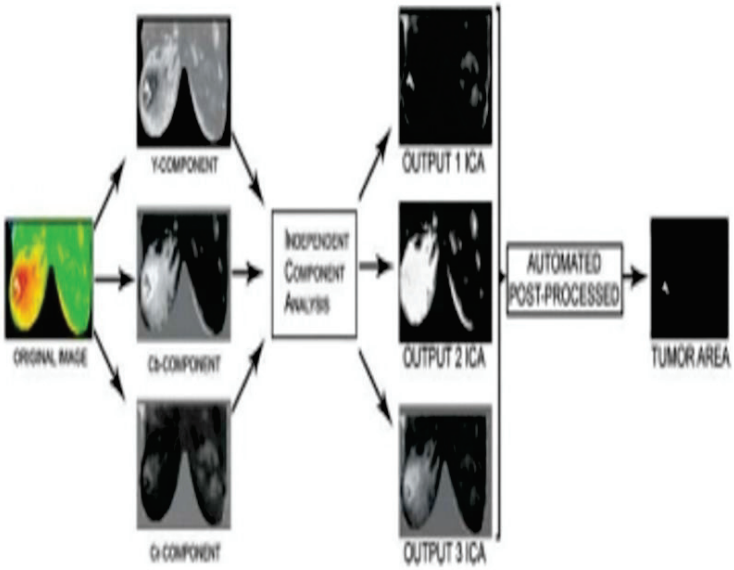

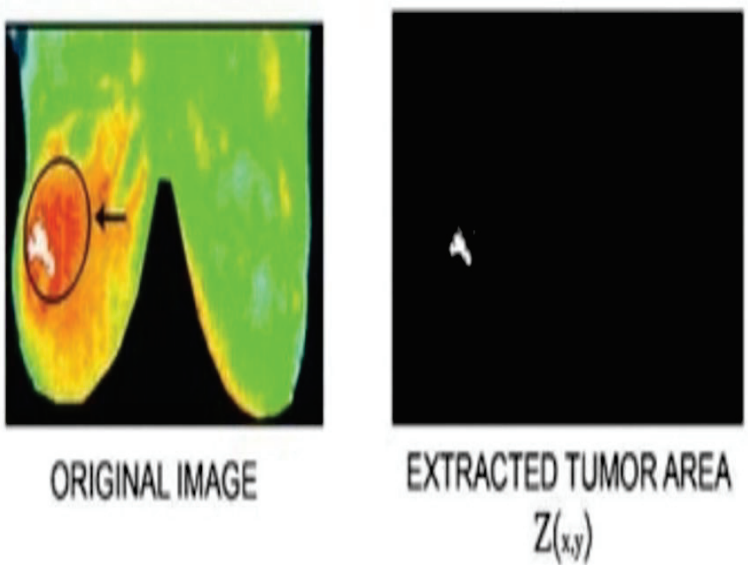

Fig .4. The ICA procedure overview in conjunction with automated post-processing, which improves the efficacy of breast tumor detection [17].

2.1.3 Lung lesion primary diagnostic:

Chengrun Li and Yang Liu published their preliminary findings in 2021 regarding the use of infrared thermography to identify intersegmental planes during lung segmentectomy in humans. Based on the features of pulmonary circulation, thermographic images that can depict a border between the ligated segments and the normal lung portion can be used to determine the difference in temperature between the surface temperatures of the segments that are being resected after the target pulmonary arteries are ligated. Thermogravimetric investigations on animal lungs have recently shown that the non-perfused lung has a lower temperature than the perfused lung; this variation in temperature can be as much as 1.5 to 2°C. For human research About three minutes after the target arteries were tied, patients' ligated region temperatures decreased by more than 2.1°C, according to infrared thermography readings. The difference will be considerably more noticeable if the surgeons inflate the lung before identifying the plane and wait for roughly five minutes, as Figure 5 illustrates [20]. In their 2017 study, Guigard S et al. employed near-infrared angiography in conjunction with a systemic injection of indocyanine green (ICG) to offer technical assistance in detecting the vasculature and intersegmental plane during VATS segmentectomy. During video-assisted thoracoscopic surgery (VATS), it improves the quality of excisions performed for diagnostic and therapeutic purposes on small nodules, which are frequently not palpable or visible [21]. Guired S. et al. (2016) came to the conclusion that near-infrared thoracoscopy (NIT) makes vascular identification easier and offers technological support for the identification of the intersegmental during VATS. It enhances the quality of segmentectomy for the excision of tiny nodules for diagnostic and therapeutic purposes, which are frequently invisible and palpable during VATS [22].

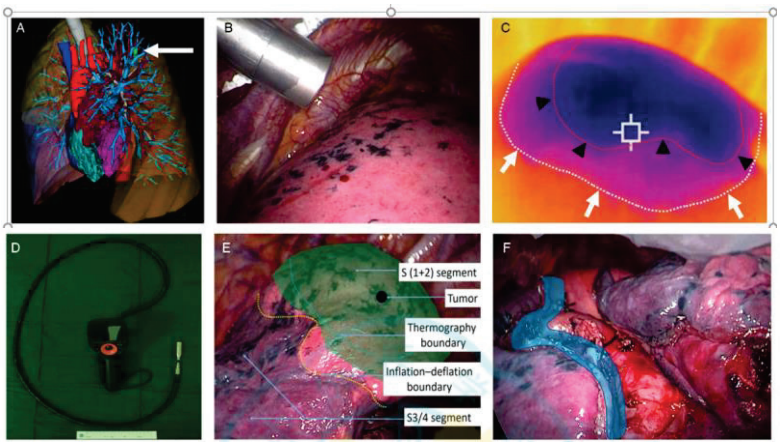

Fig .5. Tumor

Figure 5: (A) a tumor is indicated by the green hue (white arrow) in the pre-operative 3D lung reconstruction model. (B) Surgical site equipped with an infrared thermography camera. (C) The posterior and apical segmental arteries are ligated before obtaining the infrared images. The boundary between the low temperature edge zone and the normal temperature zone is shown by the white arrow as a dotted line; the boundary between the low temperature core zone and the edge zone is represented by a black arrow; and the center of vision is represented by a square. (D) Detector for infrared thermography in endoscopic mode (wavelength range: 1–20mm). (E) Infrared and inflation-deflation boundaries in the posterior and apical regions of the left upper lobe. (F) Apical and posterior segment resection along the infrared boundary (blue zone). Chinese Medical Journal 2022;135(1) www.cmj.org120© Chinese Medical Association Publishing House Downloaded from mednexus.org on [November 19, 2022]. For personal use only[20].

2.1.4 Thyroid lesion primary diagnostic.

Protocols for the capture of the thermal images and an autonomous registration for these thyroid thermographs were proposed by J. R. González et al. in 2017. In order to identify cancer early and increase the prognosis, they also conducted studies of the image data, which included feature extraction, image processing, and a potential classification of healthy or ill patients. As part of efforts to support preventative medical actions, as illustrated in Figure 6 [23], the Brazilian Ministry of Health Ethical Committee states that their study shows a valuable project for tumor identification in hospitals at Universidad Federal Fluminense (HUAP-UFF). Using Fourier transform infrared (FTIR) spectroscopy of thyroid tumor signals extracted from tissues, Santillan A et al. distinguished between benign and malignant thyroid lesions in 2021 [24].

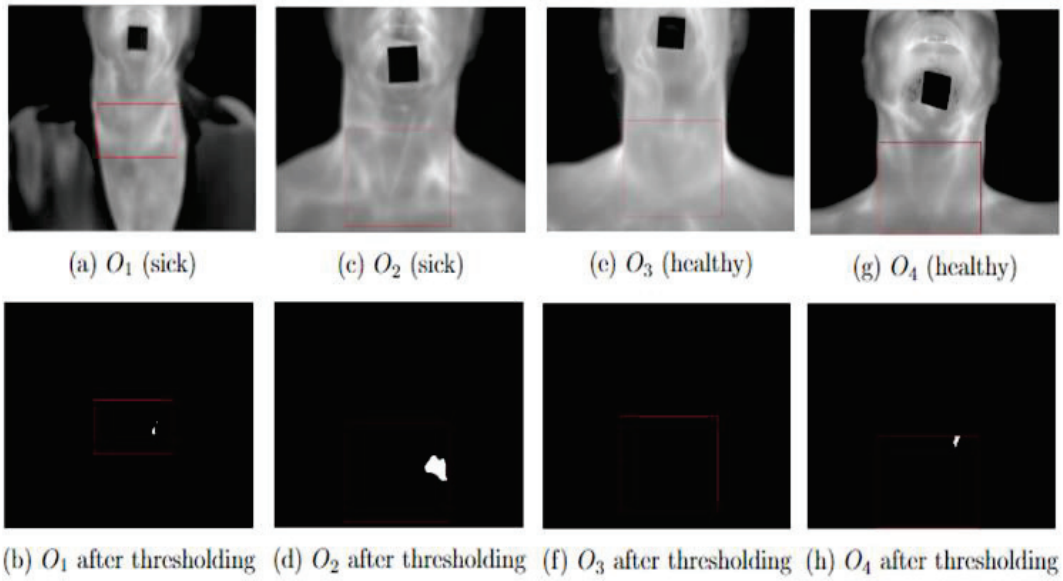

Fig .6: Temperature analysis[23].

2.2 Thermoregulation.

In 2015, Mateja Dovjak, Masanori Shukuya, and Aleš Krainer analysed the physiology of thermoregulation in various climate types using the human body exergy balance model, where the mutual influence of environmental parameters and personal factors is considered. The mutual influence of environmental parameters and personal factors on human body exergy balance (hBExB) is a key factor for identifying recommendations for healthy, comfortable, and stimulative conditions [25]. The thermoregulatory mechanisms play important roles in maintaining physiological homeostasis during rest and physical exercise. Physical exertion poses a challenge to thermoregulation by causing a substantial increase in metabolic heat production. Tympanic temperature measurement using the infrared temperature scanner. Without causing discomfort to the user, the ingestible temperature (IR) sensor can measure the user's stomach temperature with an acceptable degree of precision as a proxy measure of core temperature (Tc). In the past ten years, this method of measuring Tc has been more widely accepted and enables continuous Tc measurements in the field. Thermography, often known as infrared thermal imaging, is a method used to monitor body surface temperature in thermoregulation research. As an example, thermograms were examined to analyze distributions between central and peripheral body temperatures in extremely low birth weight infants [26], [27], [28].

Diagnosis of peripheral vascular diseases and diabetic neuropathy: Because diabetic neuropathy alters skin surface temperature, infrared thermography (IRT) is a useful diagnostic technique for diabetic neuropathy [10].

2.3 Fever screening.

The use of temperature as a scientific marker of sickness dates back to Carl Wunderlich's 1868 systematic investigation of feverish people' body temperatures and comparisons with those of healthy subjects. According to his findings, a temperature in the range of 36.3 to 37.5°C might

be regarded as normal, but any readings over this range were to be interpreted as perhaps being unwell. Liquid-based thermometers were employed in the early going. Following Sir William Herschel's 1800 discovery of infrared radiation, his son John Herschel soon after captured the first thermal image, opening up new avenues for temperature monitoring [9][29][30].

2.4 Dental diagnosis.

Dentistry has made extensive use of IRT. A new classification system for patients with persistent orofacial pain was created by Gratt et al. in 1996, utilizing thermograms. Depending on whether the temperature differential between the right and left sides was between 0 and 0.25°C, 0.35°C and less, or greater than 0.35°C, the thermograms were categorized as normal, hot, or cold. According to what they reported, the clinical diagnosis of cold thermograms is sympathetically independent pain, while the clinical diagnosis of hot thermograms is peripheral nerve-mediated pain, temporomandibular joint (TMJ) arthropathy, or maxillary sinusitis. Additional research validates the significant uses of near-infrared light transillumination in restorative dentistry [9][31][32].

2.5 Dermatological applications.

Inflammation is often the result of skin illnesses, and this aberrant temperature pattern on the skin's surface is the result. Thus, IRT could be regarded as an appropriate method for researching skin conditions. Cooler regions (such as the ear and nasal rim region) have been observed to be severely influenced by IRT, which has been utilized to diagnose leprosy subjects [9]. Thus, Barnes [10] came to the conclusion that heating the skin could reveal information about the thermal conductivities of different tissues beneath it and proposed the use of superficial heating to investigate dermatological issues [26],. This allows for the prediction of ulcers using an infrared sensor instead of more complex technology like an automatically activated integrated electro-therapy system [33] [34]. In adult and pediatric medicine, phototherapy uses infrared light (660 nm and 940 nm) wavelengths to treat dermatological illnesses, cancer, and aesthetic dermatologic issues such allergic rhinitis [35]

2.6 Blood pressure monitoring.

Cesaris et al. monitored the arterial blood pressure and corresponding thermograms in two groups of hypertensive subjects: one group received treatment with a combination of atenolol (β1 receptor antagonist) and chlorthalidone, while the other group received treatment with labetalol (mixed α/β adrenergic antagonist) and chlorthalidone. Prior to treatment, IRT was used to detect hypothermia on the hands of the participants in both groups. Following a month of therapy, the first group's peripheral vascular flow showed no changes, whereas the second group's vascular flow significantly improved [10]. The screening process for risk factors in investigations involves the use of electrocardiography (ECG) and blood tests (total cholesterol, LDL cholesterol, triglycerides, blood glucose [36], [37], [38], [39], HBA1c, C-reactive protein, urea, and electrolytes). One of the more specialized tests carried out in a primary care setting that harnesses infrared monitoring is the ankle brachial pressure index (ABPI), which calculates the blood pressure from the patient's upper and lower limbs while they are in a supine position after 10 minutes of rest [29]:

$$\text{ABPI}=\frac{*Leg\ systolic\ BP}{Hieghest\ arm\ systolic\ BP}\ [29] \tag{2.6}$$

2.7 Diagnosis of rheumatic diseases.

Schiavon G. et al. (2021) examined the usefulness of infrared thermography for the assessment of degenerative and inflammatory joint illnesses in their systemic study. Studies about the clinical utility of infrared thermography in rheumatic disorders are explained by Branco J. et al. in their systematic review published that same year. Evidence demonstrates that infrared thermography is an effective tool to assess the health status of individuals with rheumatic diseases, producing clinical information relevant to diagnosis and treatment [40] [41][42]. Optical images were obtained from the dorsal side with palmar side illumination, and a normalized Fourier transform approach was utilized to evaluate aspects regarding the spatial distribution of transmitted light along the joint. As seen in figure 7, results from a pilot investigation comprising a single time-point evaluation of 144 joints from 21 rheumatology patients showed an area under the receiver operator curve of up to 0.888 for identifying inflammation [43].

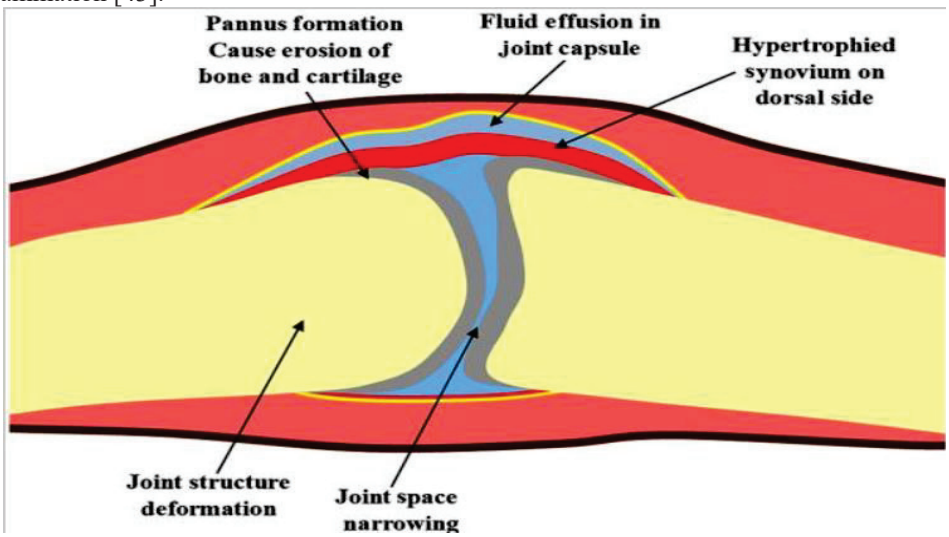

Fig .7. Illustration of the joint of an RA patient with inflammation on the dorsal side[43].

2.8 Diagnosis of dry eye and ocular diseases.

One of the main causes of dry eye disease (DE) is instability of the tear film. Ocular surface damage, visual disturbances, and optical abnormalities may be linked to the instability of the tear film. Finding evidence of tear instability in DE patients is crucial from a therapeutic perspective because particular interventions, including long-term eyelid warming therapy, may be necessary. A meaningful and quick way to evaluate pertinent features from various ocular surface regions in DE will be needed to accomplish this. Therefore, using infrared thermography images, the effectiveness of using the upper and lower half areas of the ocular surface (cornea and conjunctiva) in the identification of evaporative dry eye is evaluated in this chapter. Here, we refer to the portion of the cornea and bulbar conjunctiva that is visible when blinking naturally as the ocular surface. Participants with DE and normal eyes each get an infrared thermography photograph taken. After the first blink is segmented to receive the upper half and lower half ocular regions, discrete wavelet transforms (DWT) and Gabor transforms are utilized to extract the salient characteristics from the first, fifth, and tenth frames of the infrared thermography images. DWT is used to break down each segmented region up to three levels, and the DWT

coefficients are then subjected to the Gabor transform. To minimize the number of features, principal component analysis (PCA) is applied to the collected features. The PCA coefficients are then ranked using a t-value and supplied to an SVM classifier. We obtained classification accuracies of (i) 82.3, 89.2, and 88.2% for the left eye and (ii) 93.4, 81.5, and 84.4% for the right eye, respectively, using the first, fifth, and tenth frames of the upper half of the ocular region following the first blink. Similar results were obtained with the 1st, 5th, and 10th frames of the lower half of the ocular regions: for the left eye, the accuracy was (i) 95.0, 95.0, and 89.2%, and (ii) 91.2, 97.0, and 92.2%. In terms of DE detection using our method, this study demonstrates that the bottom part of the eye performs better than the upper half. For a quicker DE assessment, polyclinics or hospitals may use the suggested algorithm because it is effective and straightforward[44] [45]. Morgan et al. thermogrammed the ocular surfaces of individuals with dry eyes and controls using infrared radiation therapy. It was discovered that the dry eye participants' mean ocular surface temperature was higher—32.38±0.69°C—than that of the controls—31.94±0.54°C. Tan et al. have examined various approaches, including completely automatic, semi-automated, and manual techniques, for examining ocular surface temperature using infrared thermometry. Chang et al. diagnosed the inflammatory condition of patients with Graves' ophthalmopathy using IRT. The lateral orbit (reference point), upper and lower eyelids, caruncle, medial and lateral conjunctiva, cornea, and other regions were measured for temperature. It was found that temperature differences between these regions and the reference point are significantly higher in subjects with Graves' ophthalmopathy than they are in the controls. Research on the aftereffects of methylprednisolone pulse therapy has also revealed the value of IRT. During laser corneal refractive surgery, Brunsmann et al. employed IRT to assess thermal burden. An increased eye temperature may be a sign of a fever, according to Ng et al... Figure 8 shows an average thermal picture of a normal eye. The data presented in Figure (8-a) and (8-b) indicates that the distribution of corneal temperatures in healthy individuals is symmetrical, with the coolest point of the cornea being slightly away from the geometric center. The low tear fluid level is the reason for this, as it can lead to a drop in corneal warmth and the appearance of the upper eyelid.[9][46].

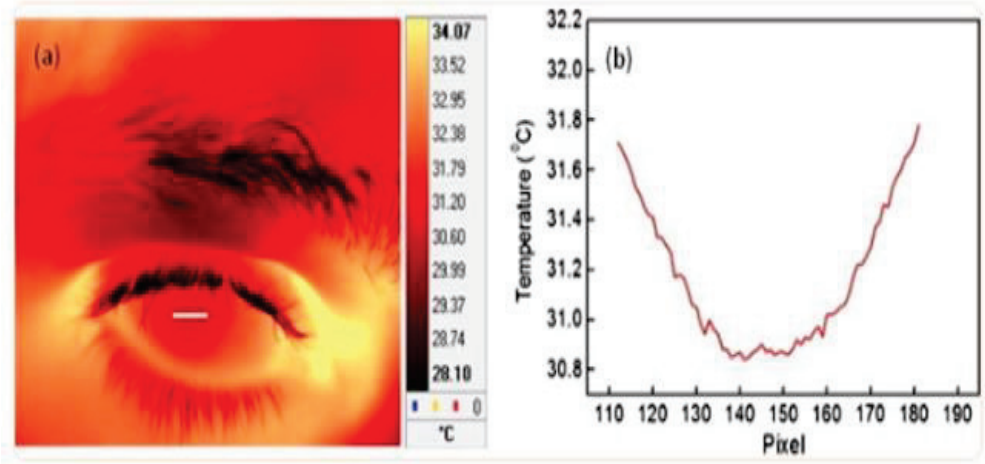

Fig .8. Thermographic (IR) image of left eye

Figure 9 (a) Thermographic (IR) image of left eye of a healthy subject, where the corneal region can be easily identified. Temperature in the cornea seems to be lower than in the surrounding area. (b) Temperature profile depicted in Fig. 8-a along the horizontal line. The line

profile demonstrates that in healthy subjects, the temperature distribution across the cornea is symmetric, and the coolest location is slightly off from the cornea's geometrical center. This could be explained by the low tear fluid, which lowers the cornea's warmth [47].

2.9 Diagnosis of liver diseases:

A variety of infrared features are used by Mansfield et al., Knobel et al., Rehman M et al., Liyanage S and Abidi N, Yang X et al. to diagnose liver abnormalities. As liver metastases result in anomalous surface temperature patterns, IRT has been utilized to detect them. Notwithstanding, IRT is also used to take the body temperature of neonates kept in incubators in order to investigate the connection between body temperature and necrotizing enterocolitis (NEC) in premature. Research has shown that premature newborns with neonatal epilepsy (NEC) have a higher mean abdominal-thoracic temperature difference. For patients with parasitic liver disorders, Milonov et al. combined thermography and electro-thermometry. Both unilocular and multilocular hydatid diseases—multilocular echinococcosis, attributed to Echinococcus multilocularis and unilocular hydatid disease, caused by Echinococcus granulosus—were identified in this investigation. Their research indicates that IRT can be a helpful method for finding suppurating cysts. According to Bhatia et al.'s IRT investigation of babies and children with acute and chronic liver disorders, 96% of the individuals had aberrant abdomen thermograms[9]. Figure 9 shows an abdomen thermogram of a hepatitis patient. The abdomen thermogram's hot spot indicates that the hepatic blood artery was obstructed after birth. The blood artery that runs from the liver to the umbilicus was opened by further measures. A system including a lens, a thermal sensor, and digital electronics processing intended for the preliminary detection of chronic liver disease was used to gather the iris images. Induced biochemical alterations in the liver are studied using Fourier transform infrared (FTIR) techniques. Two quickly developing methods that offer several advantages for the early detection, assessment, and tracking of a wide range of liver disorders are FTIR spectroscopy and micro spectroscopy imaging [45][48], [49], [50].

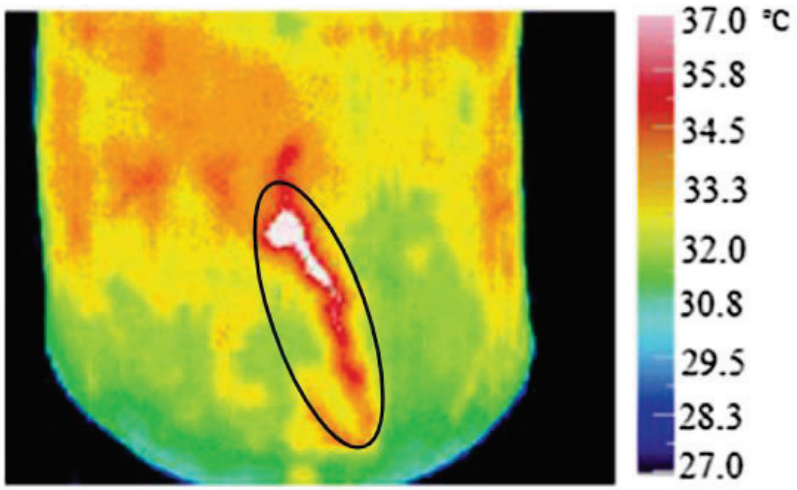

Fig .10. A patient with hepatic blood vessel blockage[45].

2.10 Treatment of kidneys:

Research indicates that IRT makes the low dispersion of hemofilters visible in real time. In order to diagnose pathological intrarenal or perirenal illnesses and assess graft function in kidney transplant recipients, Kopsa et al. determined that thermographic investigation can be a supplemental test. IRT may be useful in doing avascular plane nephrotomies with less bleeding and loss of renal parenchyma, according to Oosterlinck and De. It can also be utilized to identify distinct artery locations in the kidney. Figure 10 shows a thermogram of a patient who was complaining of back pain. Although there was no thermal evidence found in her back, her abdomen thermogram revealed small areas of hyperthermia over her right kidney, which may be related to her back pain. In addition, additional testing revealed a renal infection. In order to thermally destroy kidney cancer, multiwalled carbon nanotubes (MWCNTs) are used to produce heat in response to near-infrared radiation (NIR). This allows for the ablation of tumors with low laser powers (3 W/cm2) and very short treatment times (a single 30-sec treatment), with minimal local toxicity and no obvious systemic toxicity. In 80% of the mice administered 100 μg of MWCNT, these treatment parameters led to total tumor ablation and a prolonged remission lasting more than 3.5 months. MWCNTs combined with NIR have the potential to be useful in anticancer treatments[9] [45][48], [51].

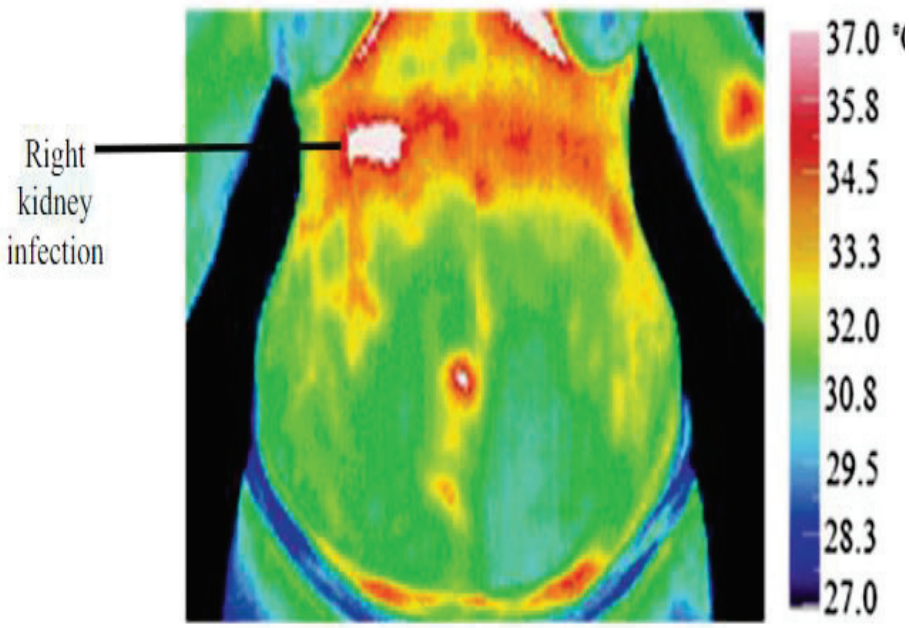

Fig .11. IR Thermography of a subject with right kidney defect confirmed with additional test[45].

2.11 Detect problems associated with heart operation:

Manginas et al. investigated thermography's viability in patients with coronary artery disease (CAD) and in patients who had heart transplants [9]. In certain Active Dynamic Thermography (ADT) applications, thermal picture capture must be timed to the patient's natural movements, which are mostly generated by breathing or, in the case of cardiovascular surgery, by heartbeat [45]. Additionally, thermography has been shown to be an early marker of a heart attack by

identifying the first indications of atherosclerosis[52]. Operational near-infrared fluorescence imaging system prototype has been employed as an extra viewing approach in many thermal operation instances[53]. Intracoronary thermography was utilized by Madjid et al. to identify susceptible, high-risk plaques[54], [55].

2.12 Detect problems associated with gynecology and neonatal physiology:

Gynecology has made considerable use of thermography as well. Gynecology, according to Birnbaum and Kliot, may have the greatest potential for using thermography because pregnancy causes major changes in the size and vascularity of the internal female genitalia, and increases the volume of the uterus, which in turn increases the number and size of blood vessels[56]. In a series of IRT tests, Menczer and Eskin assessed the temperature of female volunteers four weeks before delivery and during the first four days after delivery, both at the level of the nipples and at a set level above and below the nipples. According to a survey, those who report experiencing postpartum pain tend to have considerably higher body temperatures than those who do not[47] [57]. One of the main factors contributing to perinatal brain injury after labor is hypoxia, which also has a significant impact on the rates of morbidity, disability, and neonatal mortality. The list of mandatory birthing control measures does not include continuous infrared thermal imaging of the visible portion of the fetus's head skin after it appears as a diagnostic technique. There are no established techniques for identifying hypoxia and/or ischemia of the fetal cerebral cortex during the childbearing years. In warm-blooded mammals and humans, general and local temperature is known to play a vital role in preserving life and health. Recently, we have shown the high diagnostic value of infrared thermal imaging of different body parts surfaces for assessing hypoxic, ischemic, and drug damage in adults and children[58], [59][45].

2.13 Personality testing and brain imaging:

Functional infrared thermal imaging (fITI) is considered an upcoming, promising methodology in the emotional arena. Driven by sympathetic nerves, observations of affective nature derive from muscular activity subcutaneous blood flow as well as perspiration patterns in specific body parts[60]. According to Gulyaev et al., a subject's personality and psychological condition have an impact on their thermographic patterns. They found that temperature distributions are influenced by psychological activity, focus, and stress levels. Shevelev introduced Thermos-Encephalo-Scopy (TES), a novel technique for thermal imaging of the brain cortex, in his monograph on functional brain imaging. Neural activity, local metabolism, and local cerebral blood pressure—all of which led to measurable temperature variations—were the main processes he described for the TES process. This method identified cerebral cortex regions that were active (heated) and deactivated (cooled). He noted that activation sequences in particular cortical zones can be identified using this technique. Research shows that glial-derived brain tumors have a temperature that is 0.5–2.0°C higher than the surrounding normal tissues[47] [61][62].

2.14 Three Dimensional (3D) Dynamic Thermography System for Biomedical Applications:

A more accurate depiction of the surface temperature distribution and assistance in its interpretation are provided to users by 3D thermography systems that integrate 2D thermography data with 3D geometric data. A pair of components, one consisting of a FLIR thermal camera fixed to an off-the-shelf depth camera, is presented as a 3D dynamic infrared thermography

system. Units can be placed in desirable positions close to the patient because they are fastened to the device's arms. The information gathered from the depth cameras is matched with the thermal camera images to create a single 3D thermogram. In order to create a series of 3D thermograms, the process of creating a 3D thermogram is done multiple times while thermally stimulating the subject's surface. The created system offers several benefits for biomedical research applications, including accurate temperature readings on curved surfaces, the ability to choose regions of interest based on subject shape, and the ability to quickly remove background from 2D thermograms using 3D data [63]. As an examples for these applications are: Potentialities of Dynamic Breast Thermography, Dynamic Angiothermography (DATG), Active Dynamic Thermography in Medical Diagnostics such as skin burn diagnostics and the use of thermal imaging in cardiosurgery [45].

2.15 Potential of Thermography in Pain Diagnosing and Treatment Monitoring:

Because thermography records deep and minute temperature fluctuations, it can yield quantitative data on pain. In fact, using this approach to objectively diagnose pain can be helpful. Patients typically describe this pain as a numbness in the direction of the injured nerve, or as a flashing or intense sensation [6–8]. Regular somatic (somesthetic) pain is rarely linked to circulatory malfunction; instead, neuropathic pain is produced by thermal (Vaso-motor) changes, which are responses to the afferent noxious impulses of the unmyelinated sensory (thermoreceptor) nerves in the wall of the microvasculature. That being said, the femoral, carotid, or brachial arteries correspond to the thermal distribution of neuropathic pain. identifying and diagnosing chronic somatoform pain problems, such as determining the severity of carpal tunnel syndrome symptoms[64], [65]. Deciding on an appropriate treatment plan can be greatly aided by the differences in pathologic phases' hypo- and hyperthermic reflections seen in thermal imaging. Figure 11 is a thermography image shows pain area in patients with glover left elbow[45].

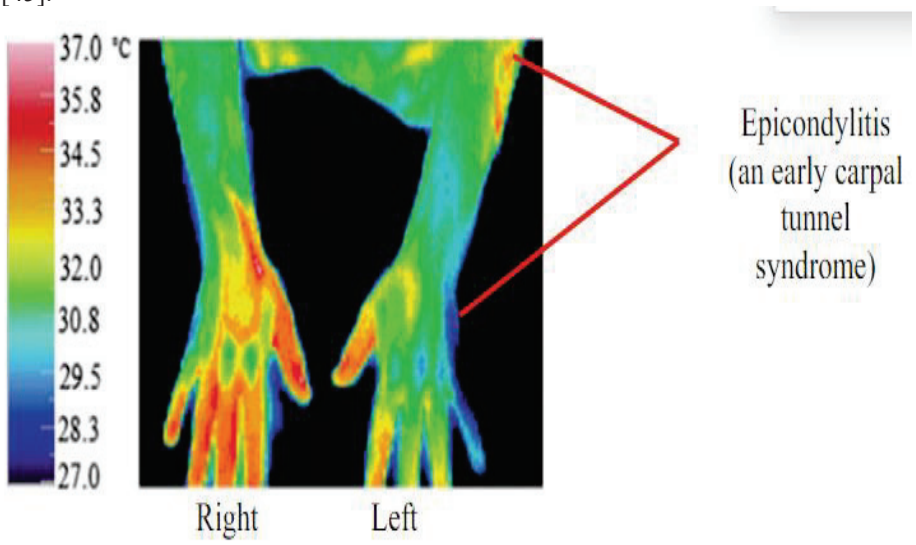

Fig .12. IR thermography of a subject suffer from golfer left elbow[45].

2.16 Physiotherapy IR applications:

invisible electromagnetic infrared radiation (IR), whose source is heated bodies and which falls between microwaves and the visible portion of red radiation in the wavelength range of 750 nm–100 μm, has gained popularity recently as a reasonably safe treatment for a number of locomotor system illnesses, as proved by Putowski M. et al. Both the beneficial heating effect, which lessens muscle tension, and local hyperemia contribute to its therapeutic effect. Moreover, IR is said to positively impact immunological responses, metabolic acceleration, pain perception (because it increases endorphin release), and autonomic nervous system activity modulation, which affects muscle tension regulation. The primary mechanism of infrared radiation at the cellular level is its interaction with water molecules [66][67].

2.17 Infrared Thermography as a Support Tool for Screening and Early Diagnosis in Emergencies:

The ability of infrared thermal imaging (IRI) to identify fever has been utilized for widespread screening in previous epidemic situations and the ongoing COVID-19 pandemic [38][68]. To be selective for the Severe Acute Respiratory Syndrome Coronavirus 2 (SARS-CoV-2) infection, a fever assessment alone might not be sufficient. Thus, new methodologies for the analysis of IRI data have been studied[69]. IRT had a good specificity for detecting temperature asymmetries on injured areas. Table 1 below shows the T_{sk} results obtained depending on the diagnosis of the injury, along with the corresponding statistical analyses (Student's t test for paired samples), comparing the injured area and uninjured region of interest ROI. The average temperatures of the skin ($T_{sk)}$ values showed significant differences between injured and uninjured ROIs ($p < 0.05$) in the case of arthrosis (ΔT_{sk}=+1.0 °C), bone fracture (ΔT_{sk}=+0.9 °C), sprain (ΔT_{sk}=+0.7 °C), meniscus injury (ΔT_{sk}=+0.7 °C), contusion (ΔT_{sk}=+0.6 °C), pain (ΔT_{sk}=+0.6 °C), synovitis (ΔT_{sk}=+0.6 °C), chondromalacia (ΔT_{sk}=+0.4 °C) and tendinitis (ΔT_{sk}=+0.4 °C). The maximum ΔT_{sk} values were significantly different in arthritis cases (ΔT_{p}=+0.9 °C), which was not observed with the average temperatures; these values were non-significant in chondromalacias and synovitis. Figure 12 below shows Data collection of the injured and non-injured ROIs [70] as shown in table 1.

Table 1 Comparison of the mean and maximal Tsk (Mean ±SD) between injured and uninjured areas by diagnosis of injury[69].

	Mean T_{sk} values (°C)					Maximal T_{sk} values (°C)				
Diagnosis (*n*)	Injured	Uninjured	ΔT_{sk}	*t*	*p*	Injured	Uninjured	ΔT_{sk}	*t*	*p*
Arthrosis (12)	32.5±1.0	31.5±0.9	**1.0**	4.01	<0.05	33.7±1.0	32.6±1.1	**1.1**	3.94	<0.05
Bone fracture (22)	32.7±1.2	31.8±1.5	**0.9**	4.54	<0.05	33.7±1.6	33.2± 1.1	**0.5**	2.11	<0.05
Sprain (25)	31.9±1.4	31.1±1.5	**0.7**	5.15	<0.05	33.1±1.3	32.5±1.4	**0.6**	3.69	<0.05
Meniscus (12)	32.0±1.4	31.3±1.2	**0.7**	3.21	<0.05	33.1±1.3	32.4±1.3	**0.7**	2.80	<0.05
Contracture (6)	32.4±0.8	31.8±1.0	**0.7**	4.87	<0.05	33.5±0.9	32.6±1.0	**0.9**	7.76	<0.05
Contussion (10)	33.2±1.1	32.6±1.1	**0.6**	4.72	<0.05	34.3±1.1	33.5±1.0	**0.7**	7.64	<0.05
Pain (no trauma) (9)	32.8±0.7	32.2±0.9	**0.6**	3.64	<0.05	33.8±0.7	33.2± 0.9	**0.6**	3.22	<0.05
Sinovitis (12)	32.5±1.3	31.9±1.4	**0.6**	2.64	<0.05	33.5±1.2	33.2±1.2	0.3	1.36	=0.20
Chondromalacia (5)	31.0±1.2	30.5±1.0	**0.4**	3.42	<0.05	32.5±0.9	31.5± 1.3	1.0	2.63	=0.06
Tendinitis (32)	32.4±1.3	32.0±1.4	**0.4**	2.78	<0.05	33.6±1.1	33.2±1.2	**0.4**	2.77	<0.05
Bursitis (4)	32.8±1.0	31.1±1.8	1.6	2.80	=0.07	34.5±0.7	32.2±1.7	2.3	2.40	=0.10
Inflamed Node (4)	32.4±0.7	31.4±1.7	0.9	1.07	=0.36	33.1±0.7	33.1±0.9	0.0	0.17	=0.87
Muscle tear (6)	31.9±1.2	31.0±0.9	0.8	1.63	=0.16	33.3±1.5	32.4±0.4	0.9	1.39	=0.23
Edema (3)	32.0±1.3	31.5±1.5	0.5	2.16	=0.16	33.0±1.1	32.3±1.4	0.7	3.95	=0.06
Arthritis (13)	31.8±1.0	31.9±2.1	–0.1	–0.13	=0.90	33.2±1.0	32.2±1.2	**0.9**	3.11	<0.05
Uncertain (22)	31.9±1.5	32.1±1.6	–0.1	–1.11	=0.28	33.1±1.2	33.3±1.3	–0.2	–1.30	=0.21
Lipoma (1)	33.6±0.0	32.4±0.0	1.2	–	–	34.4±0.0	34.1±0.0	0.3	–	–
Dislocation (1)	31.9±0.0	30.7±0.0	1.2	–	–	32.6±0.0	31.1±0.0	1.5	–	–
Periostitis (1)	32.3±0.0	32.8±0.0	–0.5	–	–	33.5±0.0	34.3±0.0	–0.8	–	–
Hernia (1)	31.1±0.0	31.9±0.0	–0.8	–	–	33.4±0.0	33.3±0.0	0.1	–	–
Total (201)	**32.3±1.3**	**31.7±1.4**	**0.5**	**7.45**	**<0.05**	**33.4±1.2**	**32.9±1.2**	**0.6**	**8.29**	**<0.05**

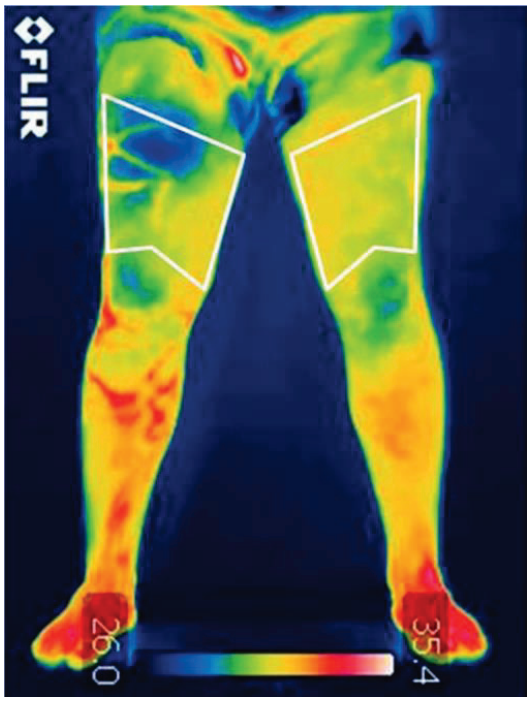

Fig .13. Data collection of the injured and non-injured ROIs (right quadriceps moderate muscle tear) [71].

Note: Nine of the patients considered "without pathology" in other Table (see table reference place) were included here into the "Pain" category and the other two were included in "Uncertain" group. The "Uncertain" group required further examinations to reach the final diagnosis.

2.18 The Application of Medical Infrared Thermography (MIT) in Sports Medicine:

MIT produced sufficiently consistent thermal patterns from the anterior knee injury, according to a research on inter-rater reliability done by Selfe et al.[72], [73]. In the field of veterinary medicine, MIT has been effectively applied to track the health and identify locomotor injuries in racehorses. Eddy et al., 2001; Turner, 2000. Turner et al. (2000) investigated tendinitis in race horses using an infrared camera, and they found hot patches prior to the appearance of swelling and lameness. Studies on human athletes are more uncommon, though. A current strategy for detecting risk factors and injury prevention should be of utmost importance in sports medicine, which aims to offer athletes with high-quality care (Bruckner & Khan, 2006). Training and competition put athletes under a lot of physical strain. The early diagnosis of overuse reactions is crucial because they are common. To choose the right course of action, it is also essential to identify inflammation early on and pinpoint its location. Normally, inflammation disrupts proper symmetry by raising skin temperature locally. A shift and a localized cooling of the affected area can also be brought on by nerve damage or disruptions to the autonomic nervous system. This method of remote sensing allows one to track changes in skin temperature brought on by exercise or therapy by measuring the body's surface temperature both during and after movement (Ring & Ammer, 1998; Hardaker et al., 2007). Sports medicine must take into account long-term, sport-specific modifications to anatomy, such as altered muscle architectures, as well as changes in physiology and, consequently, thermoregulatory functions [74]. By using

established protocols, infrared thermography (IRT) can assist in both monitoring and preventing injuries [75][76].

2.19 Near infrared (NIR) whole body imaging:

In 2012 Martha Hale reviewed the use of NIR as an excellent non-invasive technology for tracking and investigating molecular movement in vivo. Papagiannaros A. et al. in 2009 image and quantify tumors in the near-infrared region using quantum dots encapsulated in phospholipid micelles [77], [78].

2.20 Measuring Human Tissue Hemoglobin Concentration:

In 2012 Yichao Teng et al. used near infrared spectroscopy (NIRS) in continuous wave forms to detect human tissue hemoglobin concentrations. The results prove that, the in vivo calibration algorithm of measurements is effective[79].

3 Designing IR thermography

The basic components of thermographic camera based on IR detection as shown in figure 13 are:

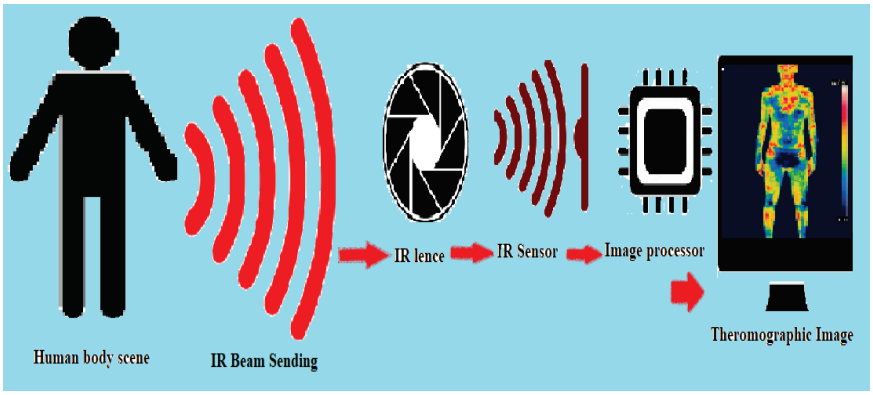

Fig .14. Basic Components of IR camera.

3.1 Infrared Optical:

There are different types of optical lenses grown from the initial areas of geometrical optics, optical detectors, and image processing to include the emerging fields of nanotechnology, biomedical optics, fiber optics, and laser technologies[80]. For a discussion of infrared optical phenomena, the classical theory of electromagnetic field propagation is generally adequate, and it is not necessary to probe the quantum nature of the pure radiation field as set out. The motion of electrons and atoms in solids, on the other hand, requires a quantum-mechanical description, although a close analogy often remains between the quantum picture of an electron making transitions between energy.

In lower or ground levels E_i and higher level $E_{j\ wich}$ is $> E_i$ and the classical picture of an electron oscillating with a frequency $\omega_{i-j} = (E_j — E_i) /\hbar$ in which $\hbar = 1.0546X\ 10^{-34}$J.s. For an atom or molecule in quantum level E_j, a transition from E_j to E_i can cause the emission of a photon

$\omega_{i-j.}$ Likewise, in the presence of an electromagnetic field of frequency ω_{i-}j, a photon can be absorbed by the system, which is correspondingly excited from level E_i to E_j. The emission process seldom occurs for completely isolated systems, although, in principle, it can. All realisable systems are bathed in radiation and interact with their surroundings.

It is found experimentally that an enclosure that forms part of a body at a uniform temperature T always contains radiation. Moreover, this radiation, if it is in thermal equilibrium with the body, has an energy distribution that depends only on the temperature T (i.e., it is independent of the material that forms the enclosure). This distribution, for temperatures at and modestly above room temperature, peaks in the infrared portion of the spectrum. It is referred to as "blackbody" radiation and is the preferred source of incoherent radiation at infrared frequencies[81].

There are two basic classifications of infrared optics:

Crystalline IR optical materials as shown in table 2.

Table 2 Crystalline Infrared Optical Materials [80], [81]: Names and Chemical Formulas

Name	Chemical Formulas	No.	Name	Chemical Formulas
ALÓN, (Raytran)	$Al_{23}O_{27}N_5$		Magnesium oxide,	MgO
Aluminum nitride	AIN		Magnesium oxide (magnesia)	MgO
Aluminum oxide (ruby)	Al_2O_3		Potassium aluminosilicate (mica)	$KAl_3Si_3O_{10}(OH)_2$
Aluminum oxide (sapphire)	Al_2O_3		Potassium bromide	KBr
Ammonium dihydrogen phosphate (ADP)	$NH_4H_2PO_4$		Potassium chloride	KC1
Barium fluoride	BaF_2		Potassium dihydrogen phosphate (KDP)	KH_2PO_4
Barium titanate	$BaTiO_3$		Potassium iodide	KI
Boron nitride	BN		Rubidium bromide	RbBr
Boron phosphide	BP		Rubidium chloride	RbCl
Cadmium fluoride	CdF_2		Rubidium iodide	Rbl
Cadmium phosphide	Cd_3P_2		Selenium	Se
Cadmium selenide	CdSe		Silicon	Si
Cadmium sulfide	CdS		Silicon carbide	SiC
Cadmium telluride	CdTe		Silicon dioxide (crystal quart)	SiO_2
Calcium carbonate, (calcite)	$CaCO_3$		Silicon nitride	Si_3N_4
Calcium fluoride	CaF_2		Silver bromide	AgBr
Calcium lanthanum sulfide,	$CaLa_2S_4$		Silver chloride	AgCl
Cesium bromide	CsBr		Sodium chloride	NaCl
Cesium iodide	Csl		Sodium fluoride	NaF
Cuprous chloride	CuCl		Strontium barium niobate	$SrBaNb_3O_6$
Diamond II A	C		Strontium fluoride	SrF_2
Gallium antimonide	GaSb		Strontium titanate	$SrTiO_3$
Gallium arsenide	GaAs		Tellurium	Te

Gallium phosphide	GaP		Thallium bromide	TlBr
Gallium selenide	GaSe		Thallium bromoiodide (KRS-5)	Tl(Br,I)
Germanium	Ge		Thallium chloride	TlCl
Indium antimonide	InSb		Titanium dioxide	TiO_2
Indium arsenide	InAs		Yttrium oxide	Y_2O_3
Indium phosphide	InP		Yttrium oxide (Raytran yttria)	Y_2O_3
Lanthanum fluoride	LaF_3		Yttrium oxide, lanthanum-doped	Y_2O_3-La
Lead fluoride	PbF_2		Zinc chloride	ZnCl2
Lead selenide	PbSe		Zinc selenide	ZnSe
Lead sulfide	PbS		Zinc selenide (CVD Raytran)	ZnSe
Lead telluride	PbTe		Zinc sulfide	ZnS
Lithium fluoride	LiF		Zinc sulfide (CVD Raytran, multispectral grade)	ZnS
Lithium niobate	$LiNbO_3$		Zinc sulfide (CVD Raytran, standard grade)	ZnS
Magnesium alumínate (spinel)	$MgAl_2O_4$		Zinc sulfide (Irtran 2)	ZnS
Magnesium alumínate (Raytran spinel)	$MgAl_2O$		Zirconium dioxide	ZrO_2
Magnesium fluoride	MgF_2		Zirconium dioxide, yttrium oxide doped	ZrO_2-Y_2O_3
Magnesium fluoride (Irtran I),	MgF_2			

Class IR optical materials as shown in table 3.

Table 3 Glass Infrared Optical Materials [80] [81]: Names and Chemical Formulas

Name	Chemical Formulas	No.	Name	Chemical Formulas
Arsenic trisulfide,	As_2S_3		Corning 9754 (germanate)	
Beryllium fluoride	BeF_2		Schott IRG 2 (germanate)	
BZYbT (fluoride)			TI 1173	$Ge_{28}Sb_{12}Se_{60}$
Schott IRG 11 (calcium alumínate)			AMTIR-1	Ge_{33} As_{12} Se_{55}
Corning 9753 (calcium aluminosilicate)				Ge_{25} Se_{75}
Schott IRG N6 (calcium aluminosilicate)			Schott IRG 100 (chalcogenide)	
Ohara HTF-1 (fluoride)			HBL (fluoride)	

Schott IRG 9 (fluorophosphate)			Schott IRQ 3 (lanthan dense flint)	
SiO2 (fused silica)			Schott IRG 7 (lead silicate)	
Corning 7940 (fused silica)			Corning 7971 (titanium silicate)	
Corning 7957 (fused silica)			ZBL (fluoride)	
Corning EO (GaBiPb oxide)			ZBLA (fluoride)	

3.2 Infrared (IR) Sensors (Detectors).

A radiation-sensitive optoelectronic component having spectral sensitivity in the infrared wavelength range of 780 nm to 50 µm is called an infrared sensor (IR sensor). Three fundamental laws of physics govern how infrared sensors function:

Planck's law of radiation: Radiation is released by any object whose temperature is not equal zero Kelvin (K).

Stephan Boltzmann's law: The absolute temperature of a black body is correlated with the total energy it emits at all wavelengths.

Wein's law of displacement: Spectra emitted by objects with varying temperatures have peaks at various wavelengths that are inversely related to the temperature.

Based on the presence of IR sources, IR sensors can be classified as:

3.2.1 Active sensors:

Consist of a receiver and a transmitter. The LED or laser diode primarily functions as a source, with the laser diode being utilized for the image and the LED for the non-image IR sensor. The energy that the detector collects and detects is emitted by the active infrared sensor, which then processes the energy further to extract the required data from the signal processor. Beam-break and reflection sensors are examples of active infrared sensors[82].

3.2.2 Passive sensors:

Only possesses detectors. The transmitter component is absent. As a source and transmitter, they employ the object. The infrared receiver picks up energy that the object produces. To get the required information, the signal processor evaluates the signal. Bolometers, thermocouples, pyroelectric detectors, and other devices are examples of passive infrared sensors. Thermal and quantum are the two categories of passive infrared sensors. The wavelength-independent thermal infrared sensors use heat as their energy source and have a slow detection and response time. Wavelengths are necessary for quantum infrared sensors, which also have quick detection and response times. For an accurate measurement, they must be cooled often [81][83]. Listed below in table 4 are the main types of detectors used in IR cameras and their advantages and disadvantages [84]– [86].

Table 4 Advantages and disadvantages of detectors used in IR cameras[87].

No.	Detector type	Advantages	Disadvantages

1	Indium Gallium Arsenide (InGaAs)	Superior quality dopants and materials, cutting edge technology, and elevated D* values at room temperature.	Constrained detection range; challenging to create consistent, high-performing arrays sensitive to wavelengths greater than 1.7 mm.
2	III–V Indium Antimonide (InSb)	Excellent dopants and materials, cutting-edge technology, and potential monolithic integration.	Heteroepitaxy with high lattice mismatch.
3	Quantum Well Infrared Photodetector (QWIP)	mature material growth, strong consistency over a wide region, and detectors with several colors.	This is not a broad spectral tuning range camera due to its low quantum efficiency, complex construction and growth, and limited range inside a specially constructed material.

The fundamental block diagram for turning infrared radiation into a video sequence is depicted in Figure 14 below. It is made up of an infrared source, transmission system, optical system, focal plane array (PPA), readout integrated circuit (ROIC), and signal processing unit [88].

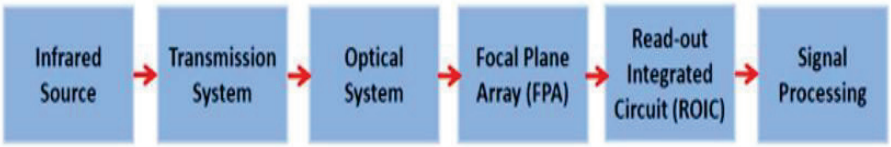

Fig .15. Converting IR radiation to IR video sequence[88]

3.3 Focal Plane Array (FPA):

An array of light-sensing pixels at a lens's focal plane makes up an FPA, an image sensing device. While they can also be utilized for non-imaging applications like spectroscopy, Light Detection and Ranging (LIDAR), and wave-front sensing, FPAs are mostly employed for imaging applications. The component that transforms infrared photons into electrical charges is referred to as the FPA in infrared imaging. IR detectors are arranged in a grid to form the FPA. A photodetector that is sensitive to infrared radiation is called an infrared detector. Thermal and photonic detectors are the two primary categories of infrared detectors [88].

Depending on the spectral region, and even in the same region, there are many different types of IR FPAs that includes[85]:

Indium antimonide (InSb).
Platinum silicide (PtSi).
Indium gallium arsenide (InGaAs).
Germanium (Ge).
Mercury cadmium telluride (HgCdTe).
Quantum well infrared photodetectors (QWIPs).

3.4 Readout Integrated Circuit (ROIC):

The circuits of the silicon chip known as the ROIC are in charge of multiplexing, amplifying, and integrating the weak detector charges. The signal processing unit and FPA are interfaced by the readout circuit [88].

The electrical contact between the individual detector elements (pixels) and the matching ROIC input unit cells is provided by an array of indium bumps connecting the ROIC and FPA. The matching unit cell integrates and samples the tiny current caused by the infrared light. Next, using a control circuit, the unit cell outputs are swept row by row and transformed into a serial stream of bits. After that, the processing unit receives this serial stream for postprocessing and anti-aliasing. The connection between a single detector in the FPA and its matching unit cell in the ROIC is illustrated by the indium bump in Figures (15) and (16) below [89].

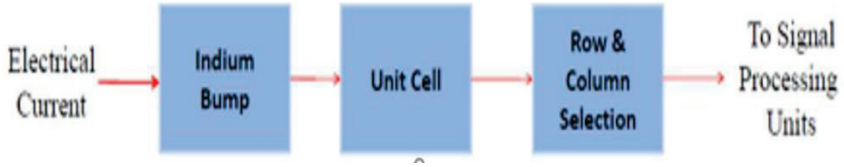

Fig .16. General block diagram of a ROIC[88].

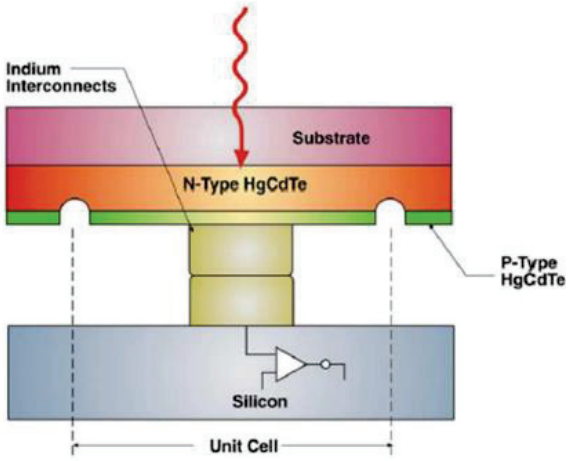

Fig .17. An Indium bump is used to connect a single detector to the unit cell [88].

There are two general classifications for IR detectors readout:

3.4.1 Photon Detectors Readouts:

Usually, photon detectors are put together in a hybrid configuration, as seen in Figure 17. An indium bump connects each pixel in the detector array to the readout's unit cell. A gentle, low-temperature metal connection between the detector and the input circuit of the readout is made possible by indium bumps. Depending on the readout architecture, two readout modes are used [90]:

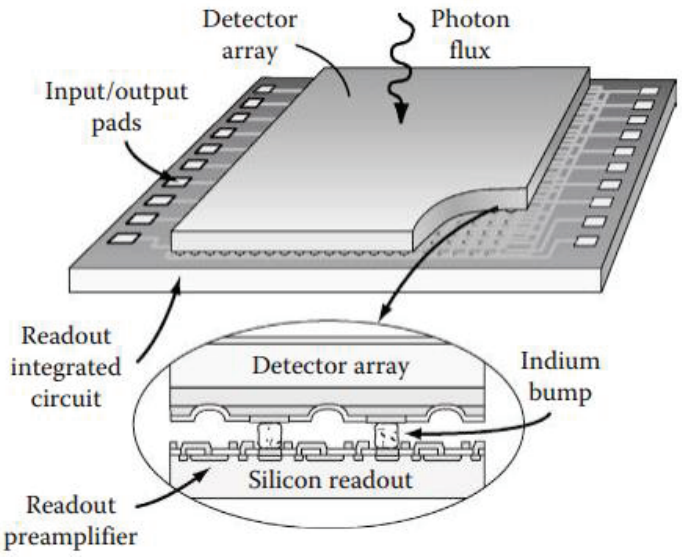

Fig .18. detector array coupled to a readout array

Figure 19 A detector array coupled to a readout array including indium metal bumps makes up a hybrid detector array construction. While photo-capacitors are occasionally employed, photodiodes or photoconductors are the most common types of detector elements. In order to integrate the optical signal, each pixel in the readout has at least one addressable switch and, more frequently, a preamplifier or buffer in addition to a charge storage capacitor[91].

a. Snapshot Modes.

These include resetting the integration capacitors after all pixels integrate simultaneously, are stored, and are then read out sequentially. Each row's capacitors in rolling frame mode are reset upon reading each pixel in that row. Here, every pixel merge into various regions of the image frame.

b. Rolling frame.

In this method, the odd rows are read in the following frame after the even rows are read out in the first.

Note: The ability to operate at greater frame rates on a subset of the entire array is known as windowing, and it is a frequent feature present on several readouts. This feature makes it possible to gather data on a constrained area of the image more rapidly.[91].

3.4.2 Thermal Detector Readouts.

Bolometer detectors have slower intrinsic reaction times and less resistance than photon detectors. This condition permits readouts that only need to sample the charge for a short period of time, rather than integrating it during the frame. Pulse-biased is a common term used to describe this mode. The lone switch in the bolometer's unit cell is pulsed on once every frame, enabling current to flow sequentially from each row to the column amplifiers. It is the row multiplexer's bias. Typically, sample times for each detector are calculated by dividing the number of rows by the order of the frame time. In order to remove a significant portion of the current flowing when the element is biased, a dummy or blind bolometer element is simultaneously supplied as an input into differential input column amplifiers, which are used in

many designs. The rolling frame readout mode is the result of the bolometer's operational design. For input to TV-like monitors, some systems additionally offer interlaced outputs [91][92].

3.5 Displayer (Thermal Imager) [1]:

A color high resolution monitor could be used to display the image, usually ≥ 12-inch square monitor such as personal computer monitor or laptop monitor[89], [93].

4 Other forms or types of IR thermography medical applications.

1. Physiotherapy
2. Temperature measurement applications (COVID 19 primary diagnostic).
3. Laboratory analysis and measurements such as spectroscopy. Important example is diagnosing acute lymphoblastic leukemia from disease free bone marrow samples[94].
4. Endoscopy lighting
5. Miscellaneous

5 Opportunities and future direction of medical IR thermography applications [2]:

Detecting infrared light that is directly connected to a specific bodily region's temperature distribution Changes in blood flow following an injury are frequently linked to changes in skin temperature. Hyperthermia is caused by inflammation, while a hypothermic pattern can be brought on by degeneration, decreased muscle activity, and inadequate perfusion.

Neurological problems are just one of the many areas in which MIT is applied in human medicine.

1. Open- heart surgery.
2. vascular diseases.
3. Reflex sympathetic dystrophy syndrome.
4. Urology problems.
5. Mass fever screening.
6. Evaluation of breast cancer [9]: The average sensitivity and specificity of breast thermography is 90%. One important biological marker for breast cancer is an aberrant breast thermogram. One theory is that tumors are linked to increased blood flow as a result of angiogenesis-induced vascular proliferation.
7. Musculoskeletal disorders (MSD) have also been linked to decreased skin temperature. In actuality, a chilly skin pattern surrounding ankle sprains portends a dire outcome and a protracted recuperation period.

6 Results and Discussion

A total of 43 articles and books were scanned for this list all the applications currently available in the medical field of infrared radiation, as well as some applications that are expected to be developed in the future. Compared to all these articles and books, this article is a comprehensive source of information for infrared applications in the field of medical diagnosis until the first months of 2023 compared to previous research and books that included fewer applications and did not cover recent applications such as examining patients with the Corona

pandemic and others. . Also, this study provided a simplified view of other medical applications. The research also included the basic design of the infrared examination system, and introductory notes on its components.

A type of light (or radiation) known as infrared (IR) is invisible to the naked eye. It is that region of the electromagnetic spectrum that is between radio waves and visible light, with wavelengths ranging from 0.7 to 300 micrometers, or around 1 to 430 THz.

The use of infrared imaging systems has gained popularity recently because of their successful uses in medical diagnosis and treatment. These systems, for instance, can be used for spectroscopy, remote temperature monitoring, and medical diagnosis and treatment. Radiation in the infrared portion of the electromagnetic spectrum is detected by thermal imaging cameras. The images created by such radiation are specifically referred to as thermograms. Every object that is close to room temperature emits infrared radiation, according to the black body radiation law [3]. As a result, thermography can be used to see in environments that are dark to the naked eye. Thermography makes it possible to see temperature swings because an object's radiation output is directly proportional to its temperature.

Infrared camera quality has increased dramatically in the last few years. Multi-color imaging systems are currently used instead of mono-color IR cameras to improve the quality of IR images by utilizing data from several IR bands. After some processing, the IR camera's output stream is transformed into a video stream. The focal plane array (FPA) and the readout integrated circuit (ROIC) are the two primary parts of an infrared camera system.

7 Conclusions.

IR imaging can be used in wide fields of application to improve medical diagnosis methods and some abnormality human treatment because it is safe and a property of human body. There is a great development in IR detection and readout resolution which can help in health field at a broad application which are not used yet and can be developed in the future and IR diagnostic is still in the beginning and need more studies for several applications.

8 Future development:

IR could be widely developed to be used in different field such as sport medicine to diagnose bone abnormality to diagnose flat foot and its severity and effect on human locomotion activities.

Some research uses different type of energy to inhibit microbial infections such as electrical current [95] or ultrasound [96], subsequently wide band high energy IR light could be used to inhibit some type of microbial infections.

References

1. M. Czerny, “Über Photographie im Ultraroten,” *Zeitschrift für Physik*, vol. 53, no. 1–2, pp. 1–12, Jan. 1929, doi: 10.1007/BF01339378.
2. R. Berz, D. Gesellschaft für Thermographie, and R. Helmut SAUER, “The Medical Use of Infrared-Thermography History and Recent Applications.” [Online]. Available: www.ndt.net/search/docs.php3?MainSource=61
3. E. F. J. Ring, “The historical development of thermal imaging in medicine,” *Rheumatology*, vol. 43, no. 6. pp. 800–802, Jun. 2004. doi: 10.1093/rheumatology/keg009.

4. "Thermography and radiology complimentary methods for the study of inflammatory diseases".
5. E. F. J. Ring, "The historical development of thermal imaging in medicine," *Rheumatology*, vol. 43, no. 6. pp. 800–802, Jun. 2004. doi: 10.1093/rheumatology/keg009.
6. R. K. Will, E. F. J. Ring, A. K. Clarke, and P. J. Maddison, "Infrared thermography: What is its place in rheumatology in the 1990s?," *Rheumatology*, vol. 31, no. 5, pp. 337–344, May 1992, doi: 10.1093/rheumatology/31.5.337.
7. R. Lawson, "IMPLICATIONS OF SURFACE TEMPERATURES IN THE DIAGNOSIS OF BREAST CANCER*," 1956.
8. R. Berz and H. Sauer, "Infrarot Regulations Imaging - innovative Funktionsdiagnostik für Früherkennung, Prävention und Problemfälle," *Erfahrungsheilkunde*, vol. 55, no. 5, pp. 241–250, May 2006, doi: 10.1055/s-2006-932327.
9. B. B. Lahiri, S. Bagavathiappan, T. Jayakumar, and J. Philip, "Medical applications of infrared thermography: A review," *Infrared Physics and Technology*, vol. 55, no. 4. pp. 221–235, Jul. 2012. doi: 10.1016/j.infrared.2012.03.007.
10. "Infrared Imaging in Medicine".
11. G. Chernov, V. Chernov, and M. Barboza Flores, "3D Dynamic Thermography System for Biomedical Applications," 2017, pp. 517–545. doi: 10.1007/978-981-10-3147-2_28.
12. C. Meola, "Infrared thermography in the architectural field," *The Scientific World Journal*, vol. 2013, 2013, doi: 10.1155/2013/323948.
13. E. F. J. Ring and K. Ammer, "Infrared thermal imaging in medicine," *Physiological Measurement*, vol. 33, no. 3. IOP Publishing Ltd, 2012. doi: 10.1088/0967-3334/33/3/R33.
14. K. Ammer, "The Glamorgan Protocol for recording and evaluation of thermal images of the human body." [Online]. Available: https://www.researchgate.net/publication/233420893
15. A. L. Shada, L. T. Dengel, G. R. Petroni, M. E. Smolkin, S. Acton, and C. L. Slingluff, "Infrared thermography of cutaneous melanoma metastases," *Journal of Surgical Research*, vol. 182, no. 1, p. e9, Jun. 2013, doi: 10.1016/j.jss.2012.09.022.
16. I. Lese *et al.*, "Transcutaneous sentinel lymph node detection in cutaneous melanoma with indocyanine green and near-infrared fluorescence: A diagnostic sensitivity study," *Medicine (United States)*, vol. 101, no. 36, p. E30424, Sep. 2022, doi: 10.1097/MD.0000000000030424.
17. S. J. Mambou, P. Maresova, O. Krejcar, A. Selamat, and K. Kuca, "Breast cancer detection using infrared thermal imaging and a deep learning model," *Sensors (Switzerland)*, vol. 18, no. 9. MDPI AG, Sep. 01, 2018. doi: 10.3390/s18092799.
18. S. S. Yadav and S. M. Jadhav, "Thermal infrared imaging based breast cancer diagnosis using machine learning techniques," *Multimed Tools Appl*, vol. 81, no. 10, pp. 13139–13157, Apr. 2022, doi: 10.1007/s11042-020-09600-3.
19. P. T. Hankare, "Breast abnormality based early diagnosis of breast cancer using non-invasive digital infrared thermal imaging," *Int J Med Eng Inform*, vol. 10, no. 4, 2018, doi: 10.1504/IJMEI.2018.095072.

20. C. Li and Y. Liu, "Detecting intersegmental plane in thoracoscopic segmentectomy using infrared thermography," *Chinese Medical Journal*, vol. 135, no. 1. Lippincott Williams and Wilkins, pp. 119–120, Jan. 05, 2022. doi: 10.1097/CM9.0000000000001806.
21. S. Guigard, F. Triponez, B. Bédat, J. Vidal-Fortuny, M. Licker, and W. Karenovics, "Usefulness of near-infrared angiography for identifying the intersegmental plane and vascular supply during video-assisted thoracoscopic segmentectomy†," *Interact Cardiovasc Thorac Surg*, vol. 25, no. 5, 2017, doi: 10.1093/icvts/ivx225.
22. S. Guigard, W. Karenovics, M. Licker, J. Vidal-Fortuny, and F. Triponez, "F-150PROSPECTIVE STUDY OF NEAR-INFRARED THORACOSCOPY FOR INTERSEGMENTAL PLANE IDENTIFICATION DURING VIDEO-ASSISTED THORACOSCOPIC SEGMENTECTOMY," *Interact Cardiovasc Thorac Surg*, vol. 23, no. suppl 1, 2016, doi: 10.1093/icvts/ivw260.148.
23. J. R. González *et al.*, "An Approach for Thyroid Nodule Analysis Using Thermographic Images," 2017, pp. 451–475. doi: 10.1007/978-981-10-3147-2_26.
24. A. Santillan *et al.*, "Discrimination of malignant from benign thyroid lesions through neural networks using FTIR signals obtained from tissues," *Anal Bioanal Chem*, vol. 413, no. 8, pp. 2163–2180, Mar. 2021, doi: 10.1007/s00216-021-03183-0.
25. M. Dovjak, M. Shukuya, and A. Krainer, "Exergetic issues of thermoregulation physiology in different climates," *International Journal of Exergy*, vol. 17, no. 4, 2015, doi: 10.1504/IJEX.2015.071558.
26. "Human thermoregulation and measurement of body temperature in exercise and clinical settings - PubMed".
27. "Thermoregulation and Thermography in Neonatal Physiology and Disease - Robin B. Knobel, Bob D. Guenther, Henry E. Rice, 2011".
28. H. Y. Naser, A. Q. Al-Neami, and Y. Ibrahim, "Study the effect of temperature variable on the patient with jaundice stay period inside the incubator," *Medico-Legal Update*, vol. 20, no. 1, 2020, doi: 10.37506/v20/i1/2020/mlu/194391.
29. "Application of Infrared to Biomedical Sciences Publisher: Springer Singapore Book Series : Series in BioEngineering."
30. R. Vardasca, C. Magalhaes, and J. Mendes, "Biomedical Applications of Infrared Thermal Imaging: Current State of Machine Learning Classification," MDPI AG, Oct. 2019, p. 46. doi: 10.3390/proceedings2019027046.
31. L. Iosif, C. Murariu-mǒgureanu, E. Preoteasa, M. Bărbînţă-pătraşcu, and C. Preoteasa, "INFRARED RADIATION IN DENTISTRY; MEASURING HEAT EMISSION THROUGH PASSIVE METHOD OF THERMOGRAPHY," 2021.
32. T. S. Vinothkumar, "Application of Near-infrared Light Transillumination in Restorative Dentistry: A Review," *Journal of Contemporary Dental Practice*, vol. 22, no. 11. Jaypee Brothers Medical Publishers (P) Ltd, pp. 1355–1361, 2021. doi: 10.5005/jp-journals-10024-3204.
33. L. M. McIntosh, M. Jackson, H. H. Mantsch, J. R. Mansfield, A. N. Crowson, and J. W. P. Toole, "Near-infrared spectroscopy for dermatological applications," *Vib Spectrosc*, vol. 28, no. 1, pp. 53–58, Feb. 2002, doi: 10.1016/S0924-2031(01)00165-5.

34. Z. S. Saleh, A. Q. Al-Neami, and H. K. Raad, "Smart monitoring pad for prediction of pressure ulcers with an automatically activated integrated electro-therapy system," *Designs (Basel)*, vol. 5, no. 3, Sep. 2021, doi: 10.3390/designs5030047.
35. R. Kennedy, "Phototherapy as a Treatment for Dermatological Diseases, Cancer, Aesthetic Dermatologic Conditions and Allergenic Rhinitis in Adult and Paediatric Medicine," *Life*, vol. 13, no. 1. MDPI, Jan. 01, 2023. doi: 10.3390/life13010196.
36. L. N. Bachache, J. A. Hasan, and A. Q. Al-Neami, "Acousto-optic Design to Measure Glucose Level for Diabetic Patients Non-invasively," in *Journal of Physics: Conference Series*, IOP Publishing Ltd, Mar. 2021. doi: 10.1088/1742-6596/1818/1/012147.
37. J. A. Hasan, L. N. Bachache, and A. Q. Al-Neami, "Noninvasive glucose sensing system based on modified SPO2 sensor," in *AIP Conference Proceedings*, 2021. doi: 10.1063/5.0065363.
38. L. N. Bachache, A. Q. Al-Neami, and J. A. Hasan, "NONINVASIVE ACOUSTO-OPTIC GLUCOSE SENSING SYSTEM FOR DIABETIC COVID-19 PATIENTS," 2021.
39. L. N. Bachache, J. A. Hasan, and A. Q. Al-Neam, "A Review: Non Invasive Sensing System for Detection Glucose Level," in *Journal of Physics: Conference Series*, IOP Publishing Ltd, Jul. 2021. doi: 10.1088/1742-6596/1963/1/012125.
40. G. Schiavon, G. Capone, M. Frize, S. Zaffagnini, C. Candrian, and G. Filardo, "Infrared Thermography for the Evaluation of Inflammatory and Degenerative Joint Diseases: A Systematic Review," *Cartilage*, vol. 13, no. 2_suppl. SAGE Publications Inc., pp. 1790S-1801S, Dec. 01, 2021. doi: 10.1177/19476035211063862.
41. "Clinical applicability of infrared thermography in rheumatic diseases_ A systematic review - PubMed".
42. J. H. L. Branco, R. L. L. Branco, T. C. Siqueira, L. C. de Souza, K. M. S. Dalago, and A. Andrade, "Clinical applicability of infrared thermography in rheumatic diseases: A systematic review," *Journal of Thermal Biology*, vol. 104. Elsevier Ltd, Feb. 01, 2022. doi: 10.1016/j.jtherbio.2021.103172.
43. D. Lighter, A. Filer, and H. Dehghani, "Detecting inflammation in rheumatoid arthritis using Fourier transform analysis of dorsal optical transmission images from a pilot study," *J Biomed Opt*, vol. 24, no. 06, p. 1, Jun. 2019, doi: 10.1117/1.jbo.24.6.066008.
44. A. Modrzejewska, "The role of thermography in ophthalmology," *OphthaTherapy. Therapies in Ophthalmology*, vol. 9, no. 1. Medical Education, pp. 14–21, 2022. doi: 10.24292/01.OT.291221.
45. E. Y. K. Ng and M. Etehadtavakol, "Series in BioEngineering." [Online]. Available: http://www.springer.com/series/10358
46. Q. Zhang *et al.*, "Screening Evaporative Dry Eyes Severity Using an Infrared Image," *J Ophthalmol*, vol. 2021, 2021, doi: 10.1155/2021/8396503.
47. B. B. Lahiri, S. Bagavathiappan, T. Jayakumar, and J. Philip, "Medical applications of infrared thermography: A review," *Infrared Physics and Technology*, vol. 55, no. 4. pp. 221–235, Jul. 2012. doi: 10.1016/j.infrared.2012.03.007.

48. X. Yang, Q. Ou, W. Yang, Y. Shi, and G. Liu, "Diagnosis of liver cancer by FTIR spectra of serum," *Spectrochim Acta A Mol Biomol Spectrosc*, vol. 263, Dec. 2021, doi: 10.1016/j.saa.2021.120181.
49. S. Liyanage and N. Abidi, "Fourier transform infrared applications to investigate induced biochemical changes in liver," *Applied Spectroscopy Reviews*, vol. 55, no. 9. Bellwether Publishing, Ltd., pp. 840–872, Oct. 20, 2020. doi: 10.1080/05704928.2019.1692307.
50. M. U. Rehman *et al.*, "Infrared Sensing Based Non-Invasive Initial Diagnosis of Chronic Liver Disease Using Ensemble Learning," *IEEE Sens J*, vol. 21, no. 17, pp. 19395–19406, Sep. 2021, doi: 10.1109/JSEN.2021.3091471.
51. A. Burke *et al.*, "Long-term survival following a single treatment of kidney tumors with multiwalled carbon nanotubes and near-infrared radiation," *Proc Natl Acad Sci U S A*, vol. 106, no. 31, pp. 12897–12902, Aug. 2009, doi: 10.1073/pnas.0905195106.
52. B. B. Lahiri, S. Bagavathiappan, T. Jayakumar, and J. Philip, "Medical applications of infrared thermography: A review," *Infrared Physics and Technology*, vol. 55, no. 4. pp. 221–235, Jul. 2012. doi: 10.1016/j.infrared.2012.03.007.
53. A. M. De Grand and J. V. Frangioni, "An Operational Near-Infrared Fluorescence Imaging System Prototype for Large Animal Surgery," *Technol Cancer Res Treat*, vol. 2, no. 6, pp. 553–562, 2003, doi: 10.1177/153303460300200607.
54. M. Madjid, J. T. Willerson, and S. W. Casscells, "Intracoronary Thermography for Detection of High-Risk Vulnerable Plaques," *Journal of the American College of Cardiology*, vol. 47, no. 8 SUPPL. Apr. 18, 2006. doi: 10.1016/j.jacc.2005.11.050.
55. B. D. MacNeill, H. C. Lowe, M. Takano, V. Fuster, and I. K. Jang, "Intravascular modalities for detection of vulnerable plaque: Current status," *Arteriosclerosis, Thrombosis, and Vascular Biology*, vol. 23, no. 8. pp. 1333–1342, Aug. 01, 2003. doi: 10.1161/01.ATV.0000080948.08888.BF.
56. S. J. Birnbaum and D. Kliot, "THERMOGRAPHY—OBSTETRICAL APPLICATIONS," *Ann N Y Acad Sci*, vol. 121, no. 1, pp. 209–222, 1964, doi: 10.1111/j.1749-6632.1964.tb13697.x.
57. J. Menczer and B. A. Eskin, "Evaluation of postpartum breast engorgement by thermography," *Obstetrics and Gynecology*, vol. 33, no. 2, pp. 260–263, 1969.
58. F. G. Costa, N. Hakimi, and F. Van Bel, "Neuroprotection of the perinatal brain by early information of cerebral oxygenation and perfusion patterns," *International Journal of Molecular Sciences*, vol. 22, no. 10. MDPI, May 02, 2021. doi: 10.3390/ijms22105389.
59. J. S. Wyatt, A. D. Edwards, D. Azzopardi, and E. O. R. Reynolds, "Magnetic resonance and near infrared spectroscopy for investigation of perinatal hypoxic-ischaemic brain injury," *Archives of Disease in Childhood*, vol. 64, no. 7 SPEC NO. BMJ Publishing Group, pp. 953–963, 1989. doi: 10.1136/adc.64.7_Spec_No.953.
60. S. Ioannou, V. Gallese, and A. Merla, "Thermal infrared imaging in psychophysiology: Potentialities and limits," *Psychophysiology*, vol. 51, no. 10. Blackwell Publishing Inc., pp. 951–963, 2014. doi: 10.1111/psyp.12243.

61. Y. V. Gulyaev, A. G. Markov, L. G. Koreneva, and P. V. Zakharov, "Dynamical Infrared Thermography in Humans," *IEEE Engineering in Medicine and Biology Magazine*, vol. 14, no. 6, pp. 766–771, 1995, doi: 10.1109/51.473272.
62. A. G. Markov, L. G. Koreneva, A. V. Tarasov, and P. V. Zakharov, "Influence of personality and stress on the regulation of peripheral blood flow in humans," *New Trends in Experimental and Clinical Psychiatry*, vol. 11, no. 1, pp. 13–18, 1995.
63. G. Chernov, V. Chernov, and M. Barboza Flores, "3D Dynamic Thermography System for Biomedical Applications," 2017, pp. 517–545. doi: 10.1007/978-981-10-3147-2_28.
64. [64] J. Yang, Y.-B. Lee, Y.-H. Sung, D.-J. Shin, Y.-J. Kim, and H.-M. Park, "Usefulness of infrared thermography in diagnosing and evaluating severity of carpal tunnel syndrome," *Annals of Clinical Neurophysiology*, vol. 23, no. 2, pp. 99–107, Oct. 2021, doi: 10.14253/acn.2021.23.2.99.
65. Z. Zou, S. Zeng, J. T. Tang, Z. Fan, and J. Cui, "Infrared Thermography: Clinical Value for Diagnosing Persistent Somatoform Pain Disorders?," *Pain Physician*, vol. 26, no. 5, pp. E529–E537, Sep. 2023.
66. M. Putowski *et al.*, "The use of electromagnetic radiation in the physiotherapy," 2016. [Online]. Available: www.medical-technologies.eu
67. L. Monje-Arenas and N. Pérez-Mallada, "Medical Thermography," in *Photography in Clinical Medicine*, Springer International Publishing, 2020, pp. 515–526. doi: 10.1007/978-3-030-24544-3_30.
68. L. Nasseer Bachache, A. Qusai Al-Neami, and J. A. Hasan, "Error grid analysis evaluation of noninvasive blood glucose monitoring system of diabetic Covid-19 patients," *Int. J. Nonlinear Anal. Appl*, vol. 13, pp. 2008–6822, 2022, doi: 10.22075/ijnaa.2022.6147.
69. D. Perpetuini, C. Filippini, D. Cardone, and A. Merla, "An overview of thermal infrared imaging-based screenings during pandemic emergencies," *International Journal of Environmental Research and Public Health*, vol. 18, no. 6. MDPI AG, pp. 1–12, Mar. 02, 2021. doi: 10.3390/ijerph18063286.
70. M. Sillero-Quintana *et al.*, "Infrared thermography as a support tool for screening and early diagnosis in emergencies," *J Med Imaging Health Inform*, vol. 5, no. 6, pp. 1223–1228, Dec. 2015, doi: 10.1166/jmihi.2015.1511.
71. M. Sillero-Quintana *et al.*, "Infrared thermography as a support tool for screening and early diagnosis in emergencies," *J Med Imaging Health Inform*, vol. 5, no. 6, pp. 1223–1228, Dec. 2015, doi: 10.1166/jmihi.2015.1511.
72. C. Hildebrandt, C. Raschner, and K. Ammer, "An overview of recent application of medical infrared thermography in sports medicine in Austria," *Sensors*, vol. 10, no. 5, pp. 4700–4715, May 2010, doi: 10.3390/s100504700.
73. J. Selfe, N. Hardaker, D. Thewlis, and A. Karki, "An Accurate and Reliable Method of Thermal Data Analysis in Thermal Imaging of the Anterior Knee for Use in Cryotherapy Research," *Arch Phys Med Rehabil*, vol. 87, no. 12, pp. 1630–1635, Dec. 2006, doi: 10.1016/j.apmr.2006.08.346.
74. C. Hildebrandt, K. Zeilberger, E. F. John Ring, and C. Raschner, "The Application of Medical Infrared Thermography in Sports Medicine," in *An International Perspective on Topics in Sports Medicine and Sports Injury*, InTech, 2012. doi: 10.5772/28383.

75. I. Fernández-Cuevas, J. Arnáiz Lastras, V. Escamilla Galindo, and P. Gómez Carmona, “Infrared Thermography for the Detection of Injury in Sports Medicine,” 2017, pp. 81–109. doi: 10.1007/978-3-319-47410-6_4.
76. M. Sillero-Quintana, P. M. Gomez-Carmona, and I. Fernández-Cuevas, “Infrared Thermography as a Means of Monitoring and Preventing Sports Injuries,” 2017, pp. 165–198. doi: 10.4018/978-1-5225-2072-6.ch008.
77. M. Hale, “Near infrared whole body imaging,” *Botulinum Journal*, vol. 2, no. 2, 2012, doi: 10.1504/TBJ.2012.050201.
78. A. Papagiannaros, T. Levchenko, W. Hartner, D. Mongayt, and V. Torchilin, “Quantum dots encapsulated in phospholipid micelles for imaging and quantification of tumors in the near-infrared region,” *Nanomedicine*, vol. 5, no. 2, 2009, doi: 10.1016/j.nano.2008.10.001.
79. Y. Teng, Y. Li, and X. Hou, “Non-invasive detecting human tissue hemoglobin concentrations using near-infrared spectroscopy with in vivo calibration,” *International Journal of Mechatronics and Automation*, vol. 2, no. 1, 2012, doi: 10.1504/IJMA.2012.046586.
80. A. Mann, “Infrared optics and zoom lenses.”
81. P. Klocek, “HANDBOOK OF INFRARED OPTIC AIM ATERÍAIS.”
82. Jeremy S Cook, “Understanding Active & Passive Infrared Sensors (PIR) and Their Uses _ Arrow.com,” *Understanding Active & Passive Infrared Sensors (PIR) and Their Uses*, 2018.
83. “newsletter-Issue-3.4-linked-INFRARED SENSOR – WHAT IT IS, CLASSIFICATION, HOW IT WORKS, TYPES, APPLICATIONS, A&D”.
84. A. Kylili, P. A. Fokaides, P. Christou, and S. A. Kalogirou, “Infrared thermography (IRT) applications for building diagnostics: A review,” *Applied Energy*, vol. 134. Elsevier Ltd, pp. 531–549, Dec. 01, 2014. doi: 10.1016/j.apenergy.2014.08.005.
85. C. D. Tran, “Principles, instrumentation, and applications of infrared multispectral imaging, an overview,” *Analytical Letters*, vol. 38, no. 5. pp. 735–752, 2005. doi: 10.1081/AL-200047754.
86. Yurish S, “Sensors and Biosensors, MEMS Technologies and its Applications,” 1965.
87. C. D. Tran, “Principles, instrumentation, and applications of infrared multispectral imaging, an overview,” *Analytical Letters*, vol. 38, no. 5. pp. 735–752, 2005. doi: 10.1081/AL-200047754.
88. A. Khoshakhlagh, “Design of a Readout Integrated Circuit (ROIC) for Infrared Imaging Applications,” 2011. [Online]. Available: https://digitalrepository.unm.edu/ece_etds/135
89. S. Bagavathiappan, B. B. Lahiri, T. Saravanan, J. Philip, and T. Jayakumar, “Infrared thermography for condition monitoring - A review,” *Infrared Physics and Technology*, vol. 60. pp. 35–55, 2013. doi: 10.1016/j.infrared.2013.03.006.
90. M. Diakides, J. D. Bronzino, and D. R. Peterson, *Medical infrared imaging: Principles and practices*. CRC Press, 2012. doi: 10.1201/b12938.
91. “MEDICAL INFRARED IMAGING PRINCIPLEs AND PRACtICEs.”

92. A. Rogalski, “History of infrared detectors,” *Opto-Electronics Review*, vol. 20, no. 3, pp. 279–308, 2012, doi: 10.2478/s11772-012-0037-7.
93. W. K. Wong, P. N. Tan, C. K. Loo, and W. S. Lim, “An effective surveillance system using thermal camera,” in *2009 International Conference on Signal Acquisition and Processing, ICSAP 2009*, 2009, pp. 13–17. doi: 10.1109/ICSAP.2009.12.
94. G. A. Raouf *et al.*, “Infrared spectroscopy of human bone marrow: Evidence of structural changes during acute leukemia,” *International Journal of Nano and Biomaterials*, vol. 2, no. 1–5, 2009, doi: 10.1504/IJNBM.2009.027724.
95. . Q. Alneami, E. G. Khalil, R. A. Mohsien, and A. F. Albeldawi, “Effect of Electrical Current Stimulation on Pseudomonas Aeruginosa Growth,” in *Journal of Physics: Conference Series*, Institute of Physics Publishing, May 2018. doi: 10.1088/1742-6596/1003/1/012112.
96. A. A. Q, K. E. Gh, M. R. A, A. A. F, and A. F. Albeldawi, “A Comparison of Six Ultrasound Stimulation Types on Pseudomonas Aeruginosa Growth in Vitro,” 2018. [Online]. Available: www.jbpe.org